



Article scientifique

Article

2021

Published version

Open Access

This is the published version of the publication, made available in accordance with the publisher's policy.

---

## Thiol-Mediated Uptake

---

Laurent, Quentin François Antoine; Martinent, Rémi; Lim, Bumhee; Pham, Anh Tuan; Kato, Takehiro; Lopez Andarias, Javier; Sakai, Naomi; Matile, Stefan

### How to cite

LAURENT, Quentin François Antoine et al. Thiol-Mediated Uptake. In: JACS Au, 2021, vol. 1, n° 6, p. 710–728. doi: 10.1021/jacsau.1c00128

This publication URL: <https://archive-ouverte.unige.ch//unige:152700>

Publication DOI: [10.1021/jacsau.1c00128](https://doi.org/10.1021/jacsau.1c00128)

# Thiol-Mediated Uptake

Quentin Laurent, Rémi Martinent, Bumhee Lim, Anh-Tuan Pham, Takehiro Kato, Javier López-Andarias, Naomi Sakai, and Stefan Matile\*

Cite This: *JACS Au* 2021, 1, 710–728

Read Online

ACCESS |

Metrics & More

Article Recommendations

**ABSTRACT:** This Perspective focuses on thiol-mediated uptake, that is, the entry of substrates into cells enabled by oligochalcogenides or mimics, often disulfides, and inhibited by thiol-reactive agents. A short chronology from the initial observations in 1990 until today is followed by a summary of cell-penetrating poly(disulfide)s (CPDs) and cyclic oligochalcogenides (COCs) as privileged scaffolds in thiol-mediated uptake and inhibitors of thiol-mediated uptake as potential antivirals. In the spirit of a Perspective, the main part brings together topics that possibly could help to explain how thiol-mediated uptake really works. Extreme sulfur chemistry mostly related to COCs and their mimics, cyclic disulfides, thiosulfates/-onates, diselenolanes, benzopolysulfanes, but also arsenics and Michael acceptors, is viewed in the context of acidity, ring tension, exchange cascades, adaptive networks, exchange affinity columns, molecular walkers, ring-opening polymerizations, and templated polymerizations. Micellar pores (or lipid ion channels) are considered, from cell-penetrating peptides and natural antibiotics to voltage sensors, and a concise gallery of membrane proteins, as possible targets of thiol-mediated uptake, is provided, including CLIC1, a thiol-reactive chloride channel; TMEM16F, a Ca-activated scramblase; EGFR, the epithelial growth factor receptor; and protein-disulfide isomerase, known from HIV entry or the transferrin receptor, a top hit in proteomics and recently identified in the cellular entry of SARS-CoV-2.

**KEYWORDS:** cellular uptake, membrane proteins, dynamic covalent chemistry, disulfide exchange, adaptive networks, molecular walkers, ring-opening polymerization, antivirals

## 1. INTRODUCTION

“Thiol-mediated uptake” refers to the observation that (i) cellular uptake reliably and often dramatically increases in the presence of chalcogenides (or mimics) capable of dynamic covalent exchange, usually disulfides, and that (ii) this uptake can be inhibited with thiol-reactive agents (Figure 1).<sup>1–7</sup> Thiol-mediated uptake has been around for a long time, with scattered observations coming from different fields.<sup>1,3,4</sup> Recently, it received more attention with the emergence of privileged scaffolds such as cell-penetrating poly(disulfide)s (CPDs)<sup>5</sup> or cyclic oligochalcogenides (COCs)<sup>6</sup> and the renewed interest in relation to viral entry<sup>8</sup> and antivirals, possibly including SARS-CoV-2.<sup>7</sup>

Considering the overwhelming evidence for usefulness in practice, it is surprising that little is known about how thiol-mediated uptake really works (*vide infra*).<sup>7,4</sup> It is understood that thiol-mediated uptake can be coupled to different uptake pathways. Dynamic covalent sulfur exchange cascades before or during direct translocation across the plasma membrane into the cytosol appear to dominate with synthetic delivery systems.<sup>5,6</sup> HIV entry is an established example for inhibitable dynamic covalent sulfur exchange on cell surfaces followed by membrane fusion,<sup>8</sup> while dynamic covalent sulfur exchange

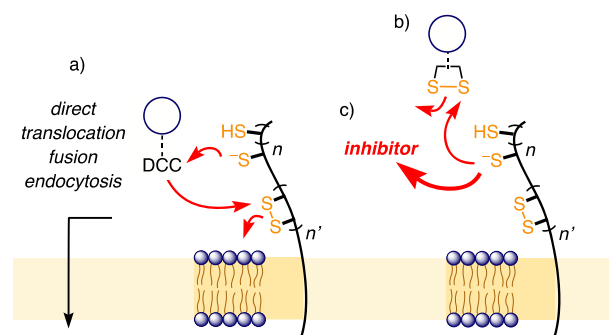
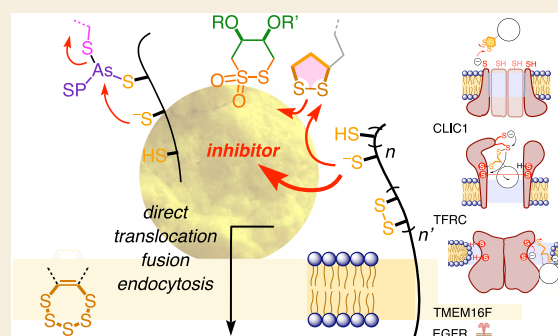
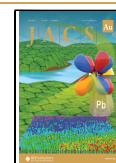


**Figure 1.** Thiol-mediated uptake (a) operates with the dynamic covalent chemistry (DCC) of chalcogenide exchange before or during cellular entry by direct translocation, endocytosis, or fusion, (b) usually involves thiol/disulfide exchange, and (c) can be inhibited with the same DCC.

Received: March 18, 2021

Published: May 3, 2021



with proteases in endosomes and lysosomes, such as cathepsins, can, perhaps, be considered as arguably borderline examples for thiol-mediated uptake combined with endocytosis.<sup>9</sup> More precise mechanistic information is often missing, particularly for direct translocation, also because dynamic covalent chemistry<sup>10–13</sup> dramatically complicates, and discourages, target identification. However, it is also this dynamic covalent chemistry that makes thiol-mediated uptake so unique and attractive, particularly from the viewpoint of supramolecular chemistry. The objective of this Perspective is, after a summary of the uptake facts available today, to map out this tantalizing chemical space surrounding thiol-mediated uptake. Topics covered are extreme sulfur chemistry, adaptive networks, thiol affinity chromatography, molecular walkers, and templated ring-opening polymerization, followed by more biological aspects such as micellar pores and a gallery of possible protein targets. Whereas only time will tell us about the direct relevance of the individual topics for thiol-mediated uptake, they are, in the spirit of a Perspective, brought up in the following to arouse curiosity and inspire progress.

## 2. CHRONOLOGY

The first explicit observation of thiol-mediated uptake was made by Ryser and co-workers in 1990 (Figure 2).<sup>1</sup> In a

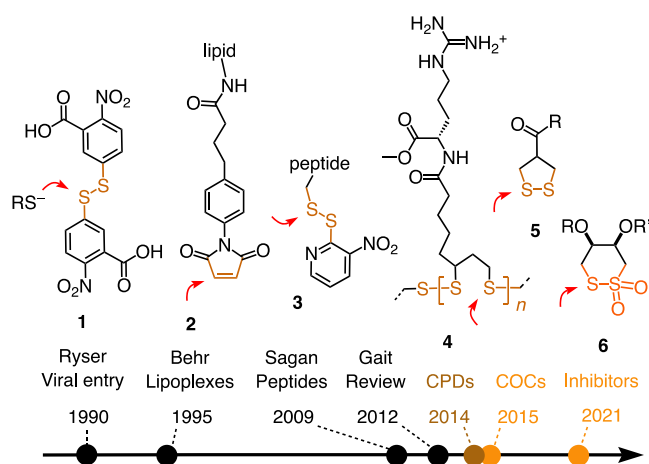


**Figure 2.** Timeline with milestones for the emergence of thiol-mediated uptake.

systematic study of uptake of disulfide-bridged drug–polylysine conjugates, inhibition by Ellman’s reagent, i.e., DTNB **1**, led to the conclusion that “the reductive properties of the cell surface may be important to maintain membrane protein sulfhydryl groups, which appear to be required for active membrane transport and for endocytosis of immune complexes”.<sup>1</sup> This breakthrough was quickly adapted to show that the entry of HIV is initiated by thiol-mediated uptake followed by fusion and can be inhibited with DTNB (see section 5.6).<sup>8</sup> The same was found early on for diphtheria toxin, followed by many examples for various microbe–host interactions (section 5.6).<sup>14</sup>

Arguably the first example for the use of thiol-mediated uptake for delivery was reported by Behr and co-workers in 1995.<sup>2,15</sup> The delivery of lipoplexes was shown to increase with various thiol-reactive agents, including disulfides, but malimide **2** was performing best (Figure 2). Thiol-mediated uptake through endocytosis was explicitly considered as a mode of action, although inhibition was not reported. Such an

inhibition with DTNB **1** was shown by Sagan and co-workers in 2009 to apply to the uptake of peptides **3** equipped with an activated disulfide.<sup>3</sup> Other scattered examples followed, mostly other peptides<sup>16,17</sup> and contrast agents,<sup>18,19</sup> together with a growing arsenal of probes to image and quantify the presence of thiols on cell surfaces.<sup>20–30</sup> However, it would be incorrect to limit thiol-mediated uptake to thiols on cell surfaces; disulfides on cell surfaces exchanging with arriving thiols are equally plausible, although clearly less considered (Figure 1a).<sup>4</sup> This also includes the possibility of exofacial disulfides in dynamic covalent exchange with substrates other than thiols. This combination is beyond the term “thiol-mediated uptake”, which is however maintained for historical reasons and the lack of convincing alternatives.<sup>4</sup> Possible contributions from glutathione (GSH) pumped from the cytosol to the cell surface, and other extracellular thiols, should not be ignored either.<sup>22,26,30,31</sup>

Besides these explicit early studies on thiol-mediated uptake, often supported by inhibition experiments, there is a remarkably rich literature that simply mentions the fact that uptake increases in the presence of chalcogenides, usually disulfides, without further explanations.<sup>4,32–51</sup> In gene transfection, disulfide polymers have been heavily explored but not with the intention to enable uptake but to degrade the transporters after uptake by reductive depolymerization in the cytosol.<sup>52–60</sup> In their seminal opinion piece in 2012, Gait and co-workers collected many of the early examples to formulate the concept of thiol-mediated uptake.<sup>4</sup>

We entered the field in 2014 by introducing cell-penetrating poly(disulfide)s (CPDs) **4**,<sup>5</sup> quickly followed by cell-penetrating cyclic oligochalcogenides (COCs) such as **5** in 2015.<sup>6</sup> More recently, COCs were found not only to activate but also to competitively inhibit thiol-mediated uptake, with thiosulfonates **6** emerging as the current best to inhibit the entry of SARS-CoV-2 lentivirus models.<sup>7</sup>

## 3. PRIVILEGED SCAFFOLDS

### 3.1. Cell-Penetrating Poly(disulfide)s (CPDs)

Coming from cell-penetrating peptides (CPPs)<sup>761</sup> and the self-organizing surface-initiated polymerization (SOSIP) of photosystems,<sup>62–65</sup> CPDs **4** have been introduced with the intention to replace their peptidic backbone with a disulfide polymer without changing the cationic side chains (Figure 3).<sup>5,66</sup> This substitution was expected, and confirmed, to minimize toxicity and endosomal capture, resulting in efficient cytosolic delivery, where the transporter is depolymerized upon arrival. Thiol-mediated uptake was supported by DTNB inhibition experiments. CPDs **4** are readily accessible by ring-opening polymerization of COC monomers, usually derivatives of lipoic acid such as **8**. In the presence of initiators such as **9–13** (Figures 3 and 4) and terminators **14** like iodoacetamide, their polymerization into CPDs **4** can occur within 5 min in neutral aqueous buffer. Interestingly, the thiolate reacts selectively with the “secondary” sulfur in monomer **8**.<sup>67</sup> Instantaneous migration to the primary sulfur proceeds until equilibrium is reached at 40% conversion, which implies that the monomers in CPDs are incorporated in a secondary/primary ratio of 6:4. With single-channel current recordings of thiolated transmembrane pores, ring-opening polymerization as well as the reverse ring-closing depolymerization could be directly observed and characterized on the single-molecule level (Figure 3).<sup>68</sup>

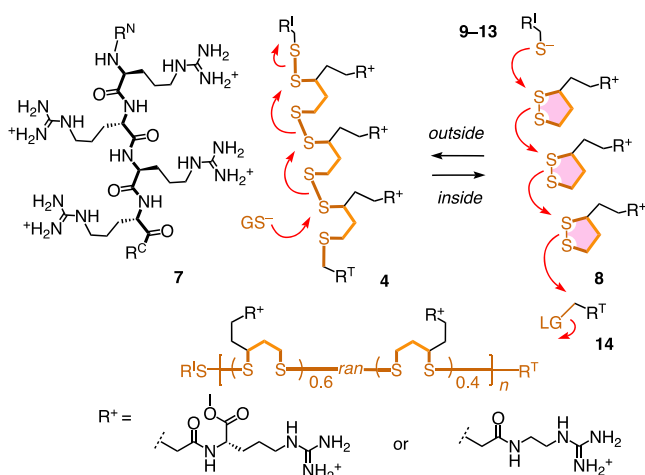


**Figure 3.** Shift of attention from CPPs 7 to CPDs 4, which are accessible *in situ* from monomers 8 and depolymerizable in the cytosol. Initiators 9–13 (see Figure 4) and terminators 14, e.g., iodoacetamide (LG, leaving group).

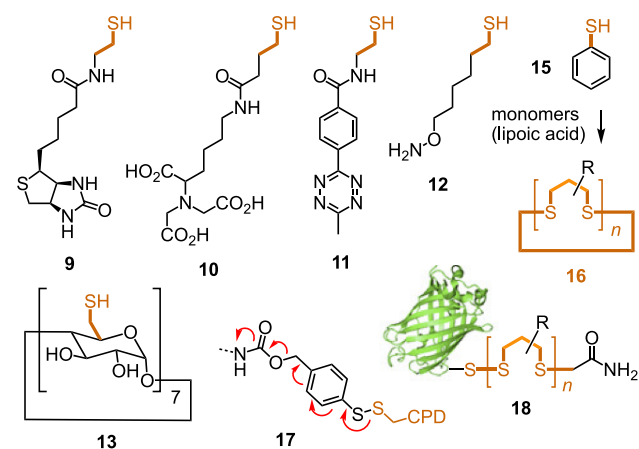


**Figure 4.** Selected CPD initiators for CPD interfacing (9–13), cyclization (15, to give 16), traceless release (17), and cryopolymerization on proteins (e.g., GFP, 18).

Further progress with CPDs focused mostly on initiators, while monomers<sup>5</sup> and terminators<sup>69</sup> received comparably little attention (Figure 4). Thiol conjugates with biotin 9, NTA 10, tetrazine 11, hydroxylamine 12, or cyclodextrin 13, mostly pioneered by Yao and co-workers, have all been introduced to interface the resulting CPDs with substrates of free choice using standard streptavidin, His-tag, IEDDA, or oxime technologies, respectively.<sup>70–77</sup> In a recent elegant study, Liu, Moore, and co-workers showed that aryl thiols 15 provide access to cyclic CPDs 16 because of the reactivity of the initial disulfide.<sup>78</sup> Traceless linkers 17 have been integrated to release native amines instead of thiols upon reductive depolymerization.<sup>77</sup> Most importantly, Lu and co-workers have shown very recently that under cryopolymerization conditions CPDs can be grown efficiently and under biorelevant conditions directly on proteins such as thiolated GFP, providing access to conjugate 18 *in situ*.<sup>79</sup>

CPDs have been used extensively to deliver a broad variety of substrates of biological interest, including probes, proteins, and so on (Figure 5). Among the more advanced systems is an artificial metalloenzyme 19 that turns on a gene switch in the cytosol for, ultimately, metabolic engineering.<sup>80</sup> Among the

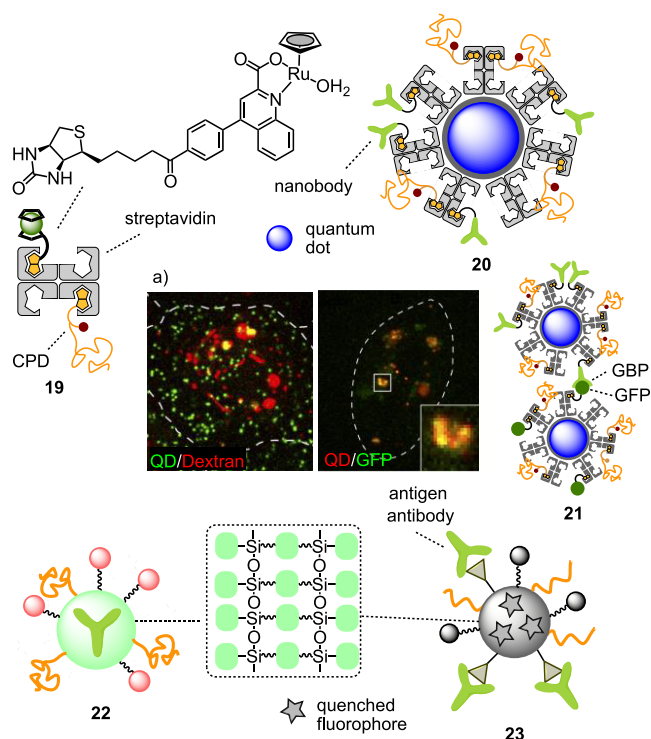


**Figure 5.** Artificial metalloenzymes (19), quantum dots (QD, 20, 21), and MPSNPs (22, 23) as selected more complex systems delivered with CPDs. (a) Microscopy images show the poor colocalization of QDs and dextran, indicating the nonendosomal localization (left), and the intracellular aggregate 21 formation by the interaction between anti-GFP nanobody (GBP) and GFP, loaded on different sets of QDs (right). Adapted from ref 81. Copyright 2017 American Chemical Society.

largest systems are quantum dots (QDs) 20, covered with streptavidin and loaded with functional nanobodies that are otherwise notoriously difficult to deliver directly to the cytosol.<sup>81</sup> The mobility analysis and the poor colocalization between QDs and fluorescently labeled dextrans demonstrated their cytosolic localization, while intracellular formation of aggregates 21 via GFP and the anti-GFP nanobody attached on the QDs showed intact functionality of the nanobodies (Figure 5a). Highlights among the extensive, creative, and highly successful studies by Yao and co-workers arguably are mesoporous silica nanoparticles (MPSNPs).<sup>71,72,75,76,82</sup> The most impressive examples include glutathione-responsive MPSNPs 22 loaded with functional antibodies and decorated with mitochondria-targeting triphenylphosphonium moieties besides CPDs<sup>75</sup> or MPSNPs 23 loaded with fluorophores and decorated with antigen/antibody complexes and fluorescence quenchers besides CPDs.<sup>72</sup> Gene transfection with CPDs obtained by templated polymerization has also been confirmed in a most elegant study by Yang, Li, and co-workers (see section 5.5).<sup>83</sup>

### 3.2. Cyclic Oligochalcogenides (COCs)

Realizing the power of thiol-mediated uptake with CPDs, we quickly shifted our attention toward COCs.<sup>6</sup> The general aim was to vary speed, selectivity, and the very nature of dynamic covalent exchange chemistry on the way into cells. COCs were selected because the released thiolates remain nearby, ready for further exchange, thus providing access to exchange cascades, adaptive networks, and so on (see sections 5.1–5.5). Initial

studies suggested that increasing ring tension in COCs correlates with increasing uptake activity.<sup>6</sup> In the relaxed disulfide **24**, an acyclic oligochalcogenide (AOC), the CXXC dihedral angle is 90°. This dihedral angle is best to minimize lone pair repulsion and maximize hyperconjugation (Figure 6).<sup>84–86</sup> In 1,2-dithiolanes **5** derived from asparagusic acid

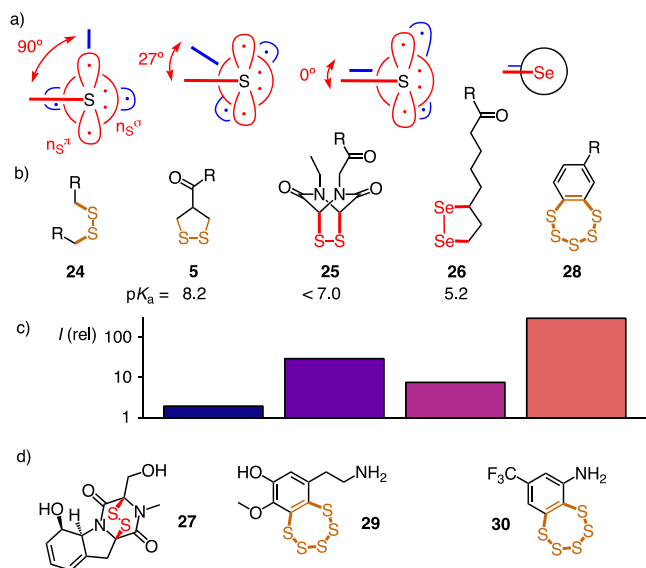


**Figure 6.** Some cyclic oligochalcogenides (COCs), highlighting (a) CXXC dihedral angles of (b) privileged scaffolds with  $pK_a$ 's of the ring-opened form, (c) their cellular uptake efficiencies,<sup>87,90</sup> and (d) their occurrence in natural products and drugs.

(AspA), the angle decreases to 27°, and in epidithiodiketopiperazines (ETPs) **25** and 1,2-diselenolanes (DSLs) **26**, the CXXC dihedral angle is around 0°. Recent studies by Raines, Movassaghi, and co-workers clarified that  $n-\pi^*$  interactions to the carbonyls stabilize ETPs sufficiently to exist under the extreme tension at 0°, while in DSLs, it is the longer Se–Se bond that makes the tension at 0° bearable.<sup>87</sup>

Like uptake activity, exchange kinetics with thiols increase with increasing tension. In the resulting ring-opened AspA **5**, the intramolecular thiol has the standard acidity of  $pK_a$  8.2 and is only marginally deprotonated in neutral water. In ring-opened ETP **25**<sup>89</sup> and DSL **26**,<sup>87</sup> the obtained thiol and selenol are much more acidic. This acidity keeps reactivity high in neutral water, including possible ring closure and release of the external thiol. This increased dynamic nature is likely to contribute to their high uptake activity (see sections 5.1–5.6).

As the name implies, AspA is a natural product found in asparagus of essentially unknown function except that the metabolites add a characteristic malodor to the urine.<sup>6</sup> ETPs also occur in natural products such as gliotoxin **27**,<sup>91,92</sup> which, interestingly, has been reported to have antiviral activity.<sup>93</sup> Benzopolysulfanes (BPS) **28** are also present in natural products.<sup>91,94,95</sup> Varacin **29**, from tunicates, an early target in total synthesis,<sup>96</sup> is arguably the most popular. BPS **30** emerged at the top of a giant library screening for kinase inhibitors involved in neurodegenerative disorder and is active in mice.<sup>97</sup> Thiol-mediated uptake of BPS **28** exceeded all other COCs (see section 5.3).<sup>90,98</sup>

Elegant studies by Wu and co-workers demonstrated that the transannular Prelog strain in  $\gamma$ -turns **31** correlates with efficient cellular uptake (Figure 7).<sup>22,102</sup> The best was a

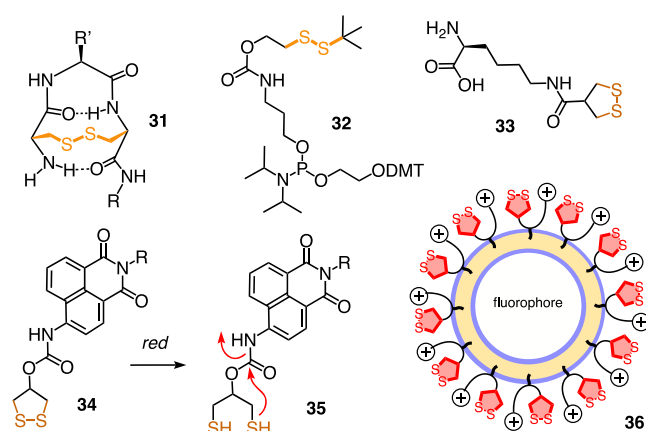


**Figure 7.** Cys-X-Cys  $\gamma$ -turns **31** as privileged COC scaffold (R = peptide, R' usually H), compatibility of COCs and AOCs with automated oligomer synthesis, and use of COCs for sensing and liposome delivery.

Cys-Gly-Cys-motif (R' = H) attached to the N-terminus of peptides, and Cys-Gly-Gly-Cys and Cys-Cys-Gly controls were less active.<sup>102</sup> While relaxed single AOCs **24** showed poor activity,<sup>6</sup> Abe and co-workers introduced phosphoramidite **32** for use in automated DNA and RNA synthesis.<sup>103–105</sup> Dependent on their positioning, the presence of 5–10 AOCs **32** resulted in efficient cytosolic oligonucleotide delivery. Peptide-based oligomers of COCs, together with the introduction of cell-penetrating streptavidin, also showed that multivalency of COCs strongly increases uptake.<sup>106</sup> The complementary AspA **33** for automated peptide synthesis has been introduced as well, and already one AspA per peptide was confirmed to suffice for efficient delivery.<sup>107</sup> 1,2-Dithiolane probes, such as **34**, that turn on fluorescence (or release drugs) upon reductive opening as outlined in **35**, have been quite extensively explored by Fang and co-workers.<sup>108–110</sup> The puzzling relation of specific thioredoxin labeling with **34** and thiol-mediated uptake is being addressed by Thorn-Seshold and co-workers.<sup>111</sup>

Like CPDs, COCs have been used to deliver a broad variety of substrates, including also artificial enzymes and quantum dots.<sup>107,112</sup> However, the largest substrates delivered in intact form to the cytosol are liposomes and polymersomes **36** of up to 400 nm diameter, loaded with internal fluorescent probes and externally added cationic COC amphiphiles.<sup>113</sup> Documenting the power and practical usefulness of thiol-mediated uptake, the different biological applications of CPDs, COCs, and AOCs have been covered in more detail in several recent reviews.<sup>70,114–119</sup>

#### 4. INHIBITORS AND ANTIVIRALS

As mentioned in the Introduction, inhibition with Ellman's reagent **1** is commonly accepted as evidence for thiol-mediated uptake (Figure 2). However, it has been noticed by several groups that DTNB inhibition is neither efficient nor reliable. The product of exchange with exofacial thiols is an activated disulfide which easily continues to exchange. We thus considered that the newly available collection of COCs could, besides containing top transporters for thiol-mediated uptake, also contain competitive inhibitors of the same process. According to the inhibition of the uptake of fluorescently labeled ETP **25** and BPS **28**, COCs are up to 5000 times better inhibitors than DTNB, with minimum inhibitory concen-

trations (MICs) reaching into the nanomolar range (Figure 8).<sup>7</sup> This result provided exhaustive support, if needed, that thiol-mediated uptake exists and is unrelated to simple passive diffusion.

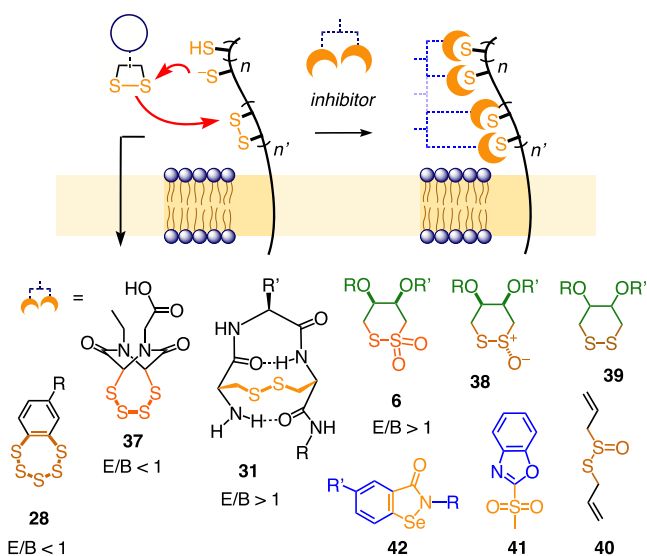


**Figure 8.** Competitive inhibitors inactivate thiols and disulfides on cell surfaces, usually by dynamic covalent chalcogenide exchange, with selected inhibitors of thiol-mediated uptake of fluorescent BPS (B, **28**, R = anionic fluorophore) and ETP (E, **25**, R = anionic fluorophore) and with indication of E/B selectivity (MICs against **25/28**).

MICs against ETP **25** (E) and BPS **28** (B) differed for every inhibitor. The resulting selectivity of inhibition can be described as the E/B ratio of the respective MICs. Different E/B values for different inhibitors supported that different uptake pathways exist for thiol-mediated uptake and that not only reactivity but also molecular recognition of and within adaptive dynamic covalent networks contribute to activity (see section 5.7). These influences beyond differences in reactivity were consistent with observations from proteomics with thiol-reactive probes.<sup>120–123</sup> About 60% of all proteins targeted by new probes differ from those targeted by established controls.<sup>120</sup>

ETP uptake was best inhibited by the expanded ETP tetrasulfide **37**, which is a relatively poor transporter.<sup>7,90</sup> Self-inhibition by ETP disulfides was almost as efficient, as was inhibition with BPS. Not surprisingly, thiol-mediated BPS uptake was generally more difficult to inhibit; i.e., E/B values were generally <1. The best inhibitors with E/B > 1 values were  $\gamma$ -turns **31**, followed by the cyclic thiosulfonate **6**. Removing oxygens from **6** to thiosulfonates **38** and DTT/DTE disulfides **39** (stereochemistry irrelevant) gradually removed inhibitory activity. The acyclic thiosulfinate allicin **40**, present in garlic, was inactive.<sup>124,125</sup> Irreversible thiol-reactive agents such as the recent **41** were moderately active inhibitors, with activity increasing with reactivity.<sup>126</sup> Ebselens **42** inhibited uptake of both probes.

Thiosulfonates **6** also inhibited the cellular uptake of SARS-CoV-2 lentivectors.<sup>7</sup> The identified IC<sub>50</sub>'s were significantly better than those measured for ebselens **42**, which have received recent attention as SARS-CoV-2 inhibitors.<sup>127–130</sup>

The cytosolic delivery by thiol-mediated uptake of CPDs or COCs is usually insensitive to inhibitors of various forms of endocytosis.<sup>5,6,74,87,89</sup> Insensitivity toward wortmannin or

cytochalasin B excludes significant macropinocytosis, chlorpromazine clathrin-mediated endocytosis, methyl- $\beta$ -cyclodextrin caveolae-mediated endocytosis, and so on.

## 5. PERSPECTIVES

Thiol-mediated uptake is attractive because it is so powerful in practice, as outlined above. Thiol-mediated uptake is tantalizing because so little is known beyond the occurrence of inhibitable dynamic covalent sulfur exchange chemistry. This poor understanding of the “sulfur magic” opens wonderful perspectives in different directions. They are outlined in the following.

### 5.1. Extreme Sulfur Chemistry<sup>131</sup>

COCs have been introduced for thiol-mediated uptake to open access to dynamic covalent exchange cascades.<sup>6,67,112</sup> With strained cyclic disulfides as substrate **5**, tension-releasing ring opening by exchange with a thiol on a cell surface, an “exofacial”<sup>4</sup> thiol, affords a new thiol in the tethered substrate next to the new disulfide bridge between the substrate and the cell. This thiol can react with a nearby exofacial disulfide (A, Figure 9a). In the resulting two-step exchange cascade, cyclic

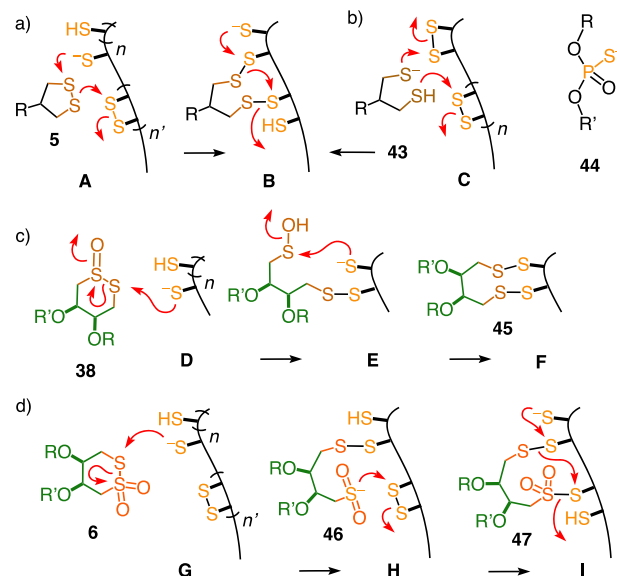


**Figure 9.** Redox-switched dynamic covalent sulfur exchange cascades of (a) disulfide COCs, covering (b) dithiols, (c) thiosulfonates, and (d) thiosulfonates. (a) Disulfides **5** can exchange with thiols, then disulfides (A), then thiols, etc (B); (b) dithiols **43**, perhaps also phosphorothioates **44**, with disulfides, etc (C, B); (c) thiosulfonates **38** with neighboring thiols (D–F); and (d) thiosulfonates **6** with thiols (G), then disulfides (H), then thiols, etc (I).

disulfides thus consume one thiol and one disulfide on the cell surface (A), build two disulfide bridges to the cell surface, and produce one new thiol (B, Figure 9a). With an additional exofacial thiol near the first disulfide formed, the exchange cascade can continue toward the next proximal disulfide (B, Figure 9a, section 5.4).<sup>67</sup> Resulting from the reduction of exofacial disulfide bridges, the neighboring thiols required to trigger continuing cascades are ubiquitous on cell surfaces.<sup>21–30</sup> The local protein misfolding caused by the exchange cascade can be expected to introduce local disorder and flexibility, which can be easily repaired after uptake via a reverse exchange cascade. Possible long-distance coupling in

exchange cascades from exofacial thiols have been indicated in pioneering early model studies on transmembrane signaling.<sup>132</sup>

In this context, disulfide COCs as in substrate **5** can be considered as hyperreactive mimics of disulfide bridges in protein substrates, with their respective selectivities added by molecular recognition. Reduction could afford 1,3-dithiols **43** already before uptake. Cascade exchange with two proximal disulfides on the cell surface (C, Figure 9b) could then yield a dynamic network that is identical with the one produced by disulfide **5** (B, Figure 9a). Such a “reversed” thiol-mediated uptake mechanism is conceivable (Figure 1a) and of interest, also considering, for example, the facile cellular uptake of phosphorothioate oligonucleotides **44** (Figure 9b).<sup>48–50</sup>

On the nondynamic sulfide level, redox switching to sulfoxide and sulfone is quite well appreciated for the rational control of structure and function.<sup>133–136</sup> On the disulfide level, the same redox switching opens attractive perspectives toward more extreme sulfur chemistry, that is, thiosulfonates **38**, thiosulfonates **6**, and beyond. Reactivity toward thiols increases with every oxygen added. Cyclic thiosulfonates **38** have been shown to selectively target neighboring thiols (D), yielding, through a sulfenate intermediate (E), two disulfide bridges **45** between the cell and substrate (F, Figure 9c).<sup>137,138</sup>

The opening of cyclic thiosulfonate substrates **6** with exofacial thiols (G) affords intermediate **46** with one disulfide bridge plus one proximal sulfinic acid in the substrate, which can continue to exchange with an exofacial disulfide (H, Figure 9d).<sup>139</sup> The net result of the full cascade is the consumption of one exofacial thiol and one disulfide, yielding macrocycle **47** with one disulfide and one thiosulfonate bridge from substrate to cell plus one new exofacial thiol (I, Figure 9d). This outcome identifies thiosulfonate COCs **6** as functional analogues of disulfide COCs **5**, including the possibility to extend exchange cascades in the likely presence of an exofacial thiol next to the disulfide bridge in I (Figure 9d). Their reactivity, however, differs significantly, according to the different functional groups involved. In small-molecule models, the formation of macrocycles **45**, sulfonates **46**, and both disulfide- and sulfonate-bridged cascade products **47** has been confirmed.<sup>137,139</sup>

These selected examples on the unfolding extreme sulfur chemistry illustrate intriguing perspectives as the COC family expands. Their development in the context of the topics that follow, from adaptive networks to templated ring-opening polymerization, promises access to diverse functions that may or may not include thiol-mediated uptake and antivirals.

## 5.2. Adaptive Dynamic Covalent Networks

The best performing BPS **28** have been introduced to drive the notion of adaptive dynamic covalent networks to the extreme (Figures 6 and 10).<sup>90</sup> Spontaneous ring contraction and expansion of the pentasulfide **28**, probably triggered by traces of thiols in the solution, have been reported by several groups and studied in more detail by Greer, Kawamura, and co-workers.<sup>95</sup> Among the identified BPS **48–53**, pentasulfide **28** is preferred, followed by trisulfide **48** and other odd-numbered rings up to nonasulfide **53**.

In the presence of thiolates and disulfides, a rich dynamic network unfolds, including besides the above BPS **48–53** also acyclic monomers **54** as well as cyclic oligomers **55**.<sup>90</sup> The largest rings observed by LC-MS are heptamers **55<sub>7</sub>** ( $m = 6$ ) with up to 19 sulfur atoms in the giant macrocycle ( $\Sigma n^x = 5$ ). From such dynamic covalent networks, cells are expected to

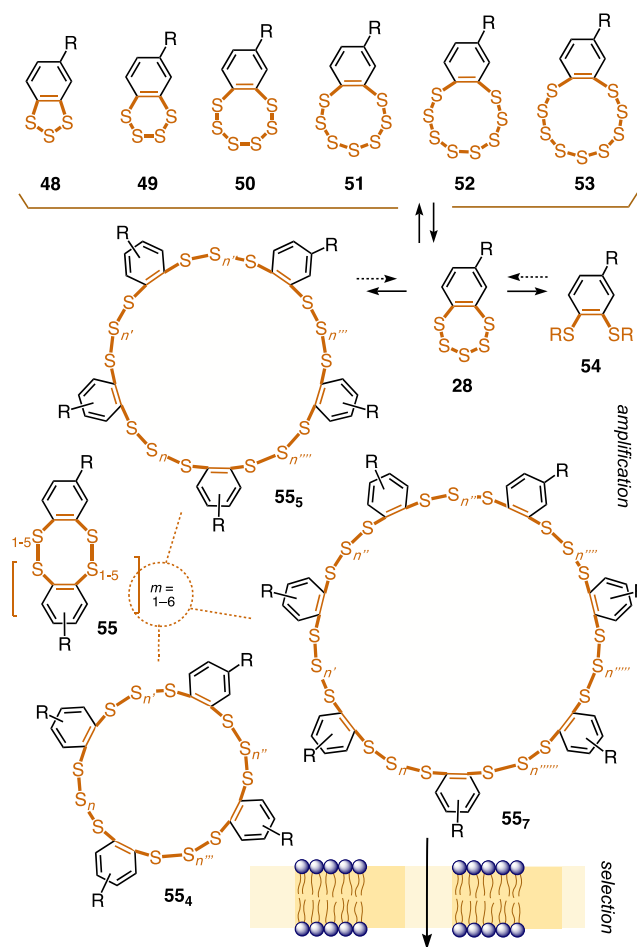


**Figure 10.** Adaptive dynamic covalent network produced by BPS **28**, with cells expected to select the best for uptake, which then will be amplified by re-equilibration.

select the best for uptake, which then could be amplified by re-equilibration of the network. This concept is as appealing as it is difficult to validate. Especially, amplification in response to uptake or different templates, including metals, remains as a most daunting challenge to tackle in future studies. The same is true for the application of the lessons learned to other COCs and the integration of techniques developed with dynamic covalent libraries.<sup>10,11</sup> These fundamental studies have provided most impressive examples for the complexity of oligomer structures that can emerge already from disulfide exchange networks.<sup>10,11</sup> Expansion into alternative reaction pathways also deserves much attention, including redox and radical chemistry, triggered by oxygen, light, and more.

## 5.3. Dynamic Covalent Affinity Columns

Thiol affinity chromatography has been considered as a convenient empirical tool to fingerprint exchange cascades and possibly mimic thiol-mediated uptake.<sup>87</sup> For fluorescently labeled 1,2-dithiolane **5**, a first fraction was directly eluted without retention (A, Figure 11a,b). A second fraction of **5** was eluted only upon addition of reduced DTT to the mobile phase. This partial retention was consistent with operational dynamic covalent exchanges on the thiolate surface of the resin, with the COC presumably being eluted in reduced form **43** (B, Figure 11a,b).

In contrast, DSL **26** was poorly retained (Figure 11c,d)<sup>87</sup> and the first fraction eluted with a slightly longer retention

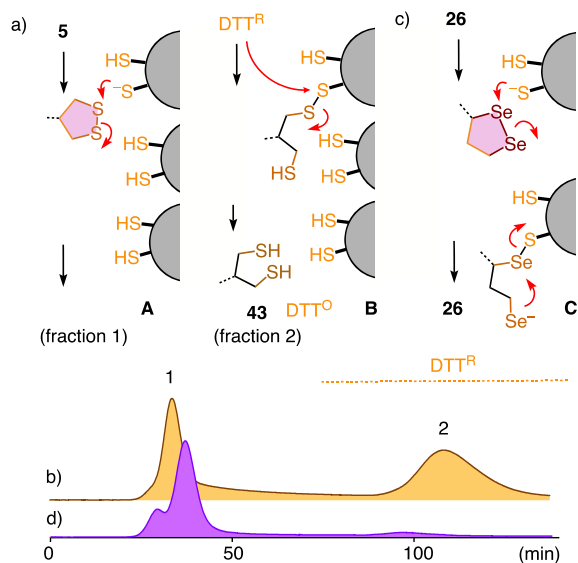


**Figure 11.** Thiol affinity columns as a tool to fingerprint dynamic covalent chalcogenide exchange networks: (a, b) After injection of AspA 5, a first fraction is eluted without retention (A), and a second fraction is eluted upon addition of DTT (B). (c, d) DSL 26 is poorly retained, presumably due to self-release by selenophilic ring closure.

time compared to that of AspA 5. These findings supported that ring opening by thiol/diselenide exchange can be followed by ring closure, with the selenophilicity of the reactive selenolate overruling the less pronounced ring tension (C, Figures 11c and 6). Although meaningful, this lack of retention obviously failed to demonstrate the occurrence of ring opening by operational dynamic covalent exchange (which was however evinced otherwise, e.g., the catalysis of DTT oxidation or trapping open reactive intermediates).<sup>67,87</sup> ETP 25 was also poorly retained on thiol affinity columns, a finding that nicely illustrates the similarity with DSL 26 with regard to the reactivity of the released thiol and possible ring closure.

Retention of BPS 28 was exceptionally strong and full elution with DTT nearly impossible, causing permanent damage to the column.<sup>90</sup> This behavior was consistent with the “sticky” adaptive network produced by BPS and differed nicely from the clean retention and release of AspA 5 on the one hand and the lack of retention with DSL 26 and ETP 25 on the other hand. Overall, thiol affinity column fingerprinting emerges as promising tool to identify the nature of different exchange cascades, which in turn are likely to provide access to different mechanisms of thiol-mediated uptake.

#### 5.4. Molecular Walkers, Pnictogens, and Conjugate Addition

The dynamic covalent exchange cascades accessible with COCs can be reminiscent of molecular walkers or hoppers. The hopping of disulfide 56 along six thiols on a  $\beta$ -sheet track inside a transmembrane  $\beta$ -barrel pore 57 has been realized by Bayley and co-workers (Figure 12a).<sup>140</sup> Equipped with a voltage-sensitive bulky DNA polyanion, the dynamic covalent exchange of disulfide 56 with the first thiol of track 57 was reported as change of the current flowing through a single pore (A, B). Exchange of the resulting disulfide with the next thiol makes the DNA hop one step forward (B, C). The directionality of further hopping along the thiol track across the pore was assured by the applied voltage (C, D, Figure 12a).

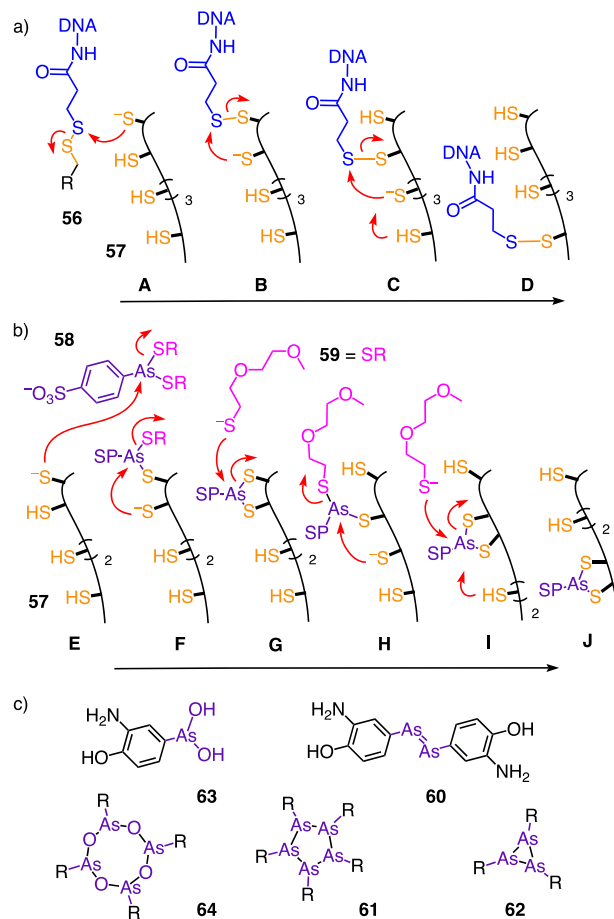


**Figure 12.** Dynamic covalent chalcogen and pnictogen exchange networks applied to molecular walkers that walk along thiol tracks 57 on a  $\beta$  sheet in a transmembrane pore. (a) A disulfide hopper 56 carrying DNA to hop by disulfide exchange cascades from the first (A, B) to the second thiol (B, C) and to the other end of the track (C, D). (b) A sulfophenyl (SP) arsonodithioite walker 58 combining chalcogen and pnictogen exchange chemistry to step on the first (E, F) and the second thiol (F, G) then moves from the first (G) to the third (H, I) and then from the second toward the terminal thiol (I, J). (c) The dynamic covalent network of Ehrlich's arsphenamine 60.

Walking instead of hopping along the same transmembrane thiol track was realized by merging dynamic covalent chalcogen and pnictogen chemistry.<sup>141</sup> Dialkyl phenylarsonodithioites 58 are well-known to covalently recognize neighboring thiols (E–G, Figure 12b). To initiate the dynamic covalent exchange cascade needed to walk along the transmembrane thiol track 57, thiol 59, reminiscent of a molecular crutch, was added. Thiolate exchange on the pnictogen center allows the crutch-supported walker to lift one foot (H), exchange with the next thiolate on the track to make one step forward (I), and so on (I, J).

This combination of dynamic covalent chalcogen and pnictogen chemistry has been used in other functional systems, such as artificial vesicles made from monomers containing three proximal thiols or polymer nanoparticles stabilized with monomers containing up to four proximal thiols.<sup>142</sup> Most significant in the present context are fluorescent arsonodithioite exchangers to dynamically label two to four neighboring thiols, the latter introduced by Tsien and co-workers as FLASH probes for the intracellular targeting of proteins with an engineered (Cys)<sub>4</sub> motif.<sup>143,144</sup> Exofacial neighboring thiols



have been imaged with such fluorescent arsonodithioite exchangers.<sup>23–25</sup> Phenyl arsine oxides were also shown early on to inhibit the entry of HIV virus about as efficiently as DTNB.<sup>8</sup> In clear contrast, thiol-mediated uptake and its inhibition remain a fascinating topic to be explored with dynamic covalent pnictogen chemistry, including possible contributions of turned-on noncovalent pnictogen bonds into deepened  $\sigma$  holes.<sup>145</sup>

Complementary to COC networks, the dynamic covalent networks accessible with pnictogens are arguably best illustrated with arsenphenamine.<sup>146</sup> Ehrlich's "magic bullet", often considered the first drug developed by dedicated SAR, has long been considered to be the azobenzene homologue **60** (Figure 12c). Only rather recent studies have indicated that **60** evolves into a collection of cyclic oligomers **61** and **62**, which then release **63**, which is considered to be the active form of the antisiphilic drug and further cyclizes into larger rings such as tetramer **64**.

Further expanding from molecular walkers that operate with dynamic-covalent chalcogen and pnictogen chemistry, divalent reversible Michael acceptors have also been considered to generate directional exchange cascades. Leigh and co-workers have realized molecular walkers **65** that walk with conjugate addition along a polyamine track **66** (Figure 13a).<sup>147</sup> Initial conjugate addition triggers the elimination of

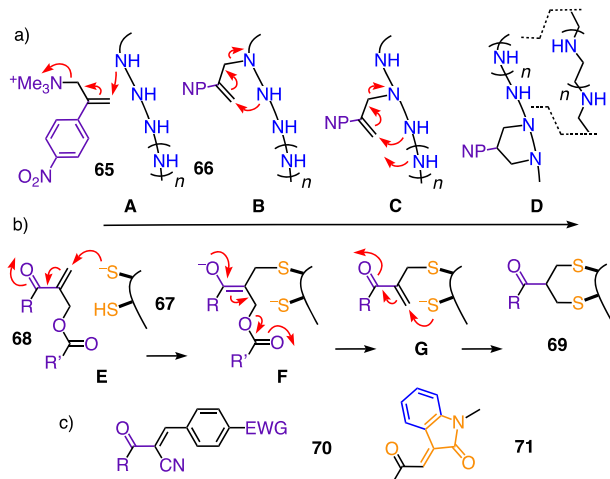


**Figure 13.** Dynamic covalent conjugate addition cascades to (a) create molecular walkers **65** that walk along polyamine tracks **66** from the first two (A–C) to the last two amines (C, D) and (b) to create molecular probes **68** that recognize neighboring thiols **67**, with addition of the first thiol (E) generating the second acceptor in situ (F) for addition to the neighboring thiols (G), producing the two, possibly dynamic sulfide bridges in product **69**. (c) Cyano and phenyl acceptors in **70** to enhance the reversibility of Michael addition cascades (EWG, electron-withdrawing group) and carbonyl acceptors in **71** to enhance the spiciness of cinnamaldehyde.

trimethylamine to yield a second conjugate acceptor (A, Figure 13a). The second amine on the track then adds to this second alkene, releasing the first amine and regenerating another alkene at the same time (B). To move forward, the third amine then adds to this alkene, and so on (C, D).

Michael cascades for thiol addition have received the most attention for the fluorescence imaging of neighboring thiols **67**, also on cell surfaces (Figure 13b).<sup>20</sup> Conjugate addition of the first thiolate to cascade probe **68** (E) produces a new acceptor

(F, G) which reacts with the second thiol (G) to end up with two sulfide bridges **69** from probe to protein. The reversibility required for dynamic adaptive networks and, perhaps, cellular uptake depends on the acidity of the  $\alpha$  hydrogens. Increasing reversibility has been obtained with cyano acceptors and  $\pi$ -acidic aromatics as in **70**, also in lipid bilayer membranes.<sup>148–151</sup>

Conjugate addition is ubiquitous in medicinal chemistry, arguably leading to the renaissance of covalent drugs. For conjugate addition to membrane proteins, activation of the spice receptor TRPA1 with cinnamaldehyde, mustard oil, or the synthetic superspice **71** is a most spectacular example (see section 5.7).<sup>152</sup> Reversible cascade Michael acceptors remain to be explored for thiol-mediated uptake, its inhibition, and the related topics outlined above.

### 5.5. Templated Ring-Opening Polymerization

In light of the different expressions of the dynamic covalent chemistry of COCs described thus far, their reversible polymerization into CPDs can be considered as a special expression of cascade exchange. From this perspective, adaptive networks translate into the templated ring-opening polymerization (TROP) of COCs (Figure 14). For TROP,

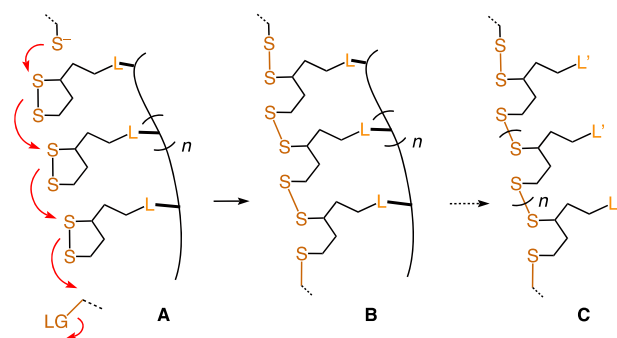


**Figure 14.** Ring-opening polymerization (ROP) of cyclic oligochalcogenides (COCs) attached with a cleavable linker L along a template.

COCs are first covalently or noncovalently interfaced with a template using a linker L (A); then the polymerization is initiated with a thiol (A, B); and then the template is detached to liberate polymers such as CPDs **4** (C, Figures 14 and 3). Templated polymerization would be of interest to control length and, at best, also sequence of the resulting polymer. While TROP has been used regularly to build functional systems with 1,2-dithiolanes (Figure 15), studies on template release (Figure 14, B, C), sequence selectivity, and eventually also self-replication remain to be realized.<sup>153</sup> ROP and TROP with other COCs are unexplored, as it is appealing not only with regard to new CPDs (Figures 3–5) but also for materials applications, dynamer plastics, and beyond.

The first systematic study on TROP with 1,2-dithiolanes was reported by Regan and co-workers, who attached lipoic acids at the end of lipid tails (Figure 15).<sup>154</sup> These artificial lipids **72** were assembled into vesicles. Their TROP was then initiated with the addition of hydrophobic thiols (Figure 15, A, B). The obtained poly(disulfide)s stabilized vesicles and were not further characterized.

Templated ROP of cationic lipoic acid derivatives on oligonucleotides has been considered early on as a strategy for gene transfection (without consideration of thiol-mediated uptake).<sup>58</sup> Monomers **8** developed for CPDs (Figure 3) were

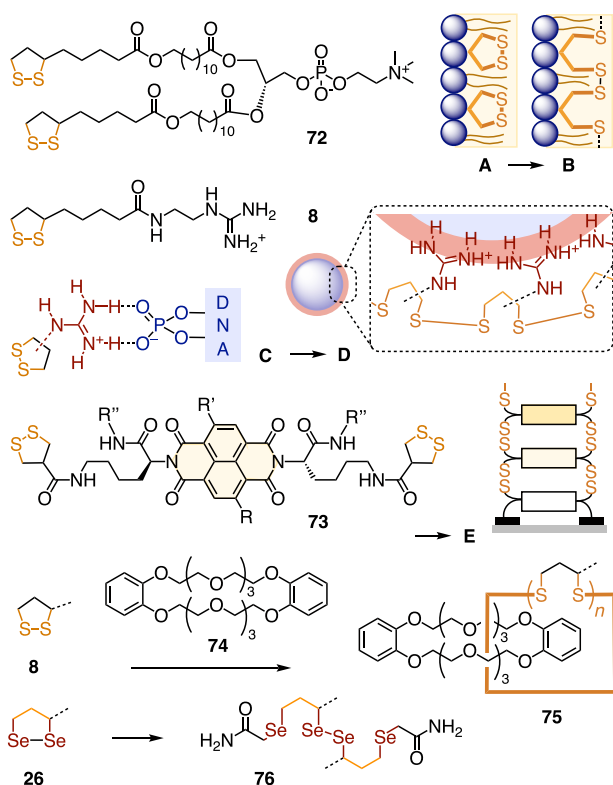


**Figure 15.** Examples for ring-opening polymerization (ROP) of 1,2-dithiolanes templated in vesicles (A, B), on DNA nanoparticles (C, D), along  $\pi$  stacks on electrodes (E) and through macrocycles 74, compared to the practically unexplored ROP of 1,2-diselenolanes 26.

studied more recently by Yang, Li, and co-workers for templated polymerization on DNA templates and gene transfection by thiol-mediated uptake (Figure 15, C, D).<sup>83</sup> Whereas uptake was excellent, separation from the template and characterization of the polymers obtained by TROP were beyond the context of the study.

Templated ROP of COC dimers such as 73 has emerged as the method of choice to grow ordered and oriented double-channel photosystems with antiparallel redox gradients on conducting surfaces (Figure 15, E).<sup>62–65</sup> Hydrogen-bonding assisted  $\pi$  stacks of the central aromatics serve to template ROP of the COCs at both sides. Evidence for operational templation has been secured by self-sorting. The resulting self-organizing surface-initiated polymerization (SOSIP) has been developed comprehensively.

Macrocycles 74 can be considered as unusual templates for ROP of lipoic acid 8 into catenated polymers 75.<sup>155</sup> In the materials sciences, nontemplated ROP of 1,2-dithiolanes is attracting increasing attention in the context of responsive dynamic-covalent materials, including “green plastics”.<sup>78,156–163</sup> COCs other than 1,2-dithiolanes were much less considered thus far for ROP, not to speak of TROP. The cyclic oligomers 55 in adaptive networks produced by BPS 28 provide an inspiring illustration for what could possibly be achieved with TROP of COCs other than 1,2-dithiolanes (Figure 10). Already TROP of 1,2-diselenolane homologues 26 will be intriguing considering their preference to stay closed. Only dimers 76 have so far been trapped during efforts to detect and characterize the opening of 1,2-diselenolanes 26.<sup>67</sup> Poly(diselenides)s have been prepared by other methods

that involve neither ROP nor dynamic covalent chalcogenide exchange chemistry and shown to penetrate cells efficiently.<sup>164</sup>

### 5.6. Micellar Pores

A central question with thiol-mediated uptake is how large substrates, from proteins to nanoparticles and liposomes, are delivered to the cytosol by mechanisms different from endocytosis, thus bypassing endosomal capture (sections 3.1 and 3.2). With CPPs, this question has arguably been answered with transient micellar pores.<sup>165</sup> It is thus not unlikely that they contribute also to thiol-mediated uptake by direct translocation across the plasma membrane into the cytosol.

Micellar pores, referred to also as lipid ion channels or toroidal pores, can form spontaneously in lipid bilayer membranes. Their saddle-shaped surface is the result of a combination of negative and positive curvature, obtained by the combination of normal (or hexagonal 1) and inverted (or hexagonal 2) micellar fragments as outlined in Figure 16.

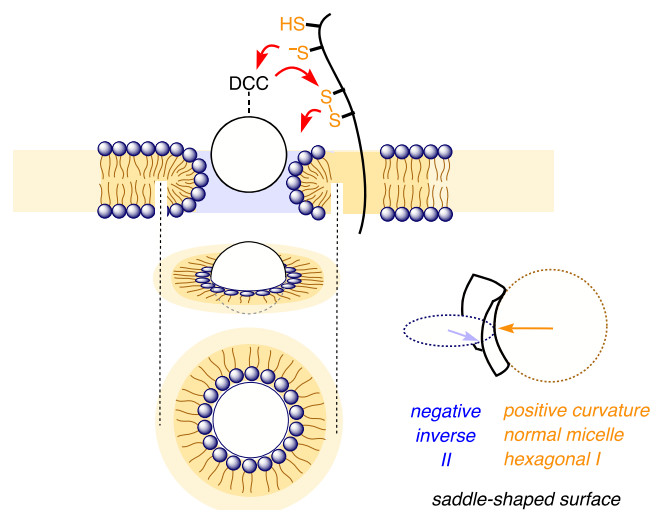


**Figure 16.** Schematic side, perspective, and top view (top to bottom) of micellar pores (or lipid ion channels, toroidal pores) next to dynamic covalent chalcogen exchange networks as outlined in preceding figures.

Observed as early as 1974,<sup>166</sup> micellar pores were characterized in detail by Heimburg and co-workers, including voltage dependence.<sup>167</sup> Colombini and co-workers reported that the presence of ceramides favors the formation of micellar pores.<sup>168</sup> Many peptides are known to induce the formation of micellar pores, including helical toxins and antibiotics. Matsuzaki and co-workers demonstrated that magainin-induced micellar pores coincide with lipid flip-flop and can be characterized with the respective assays.<sup>169</sup> Micellar pores have also been proposed to explain ion channel formation by transmembrane B-DNA helices.<sup>170</sup>

The formation of micellar pores by CPPs has been demonstrated with single-channel conductance experiments and supported by computational models.<sup>171,172</sup> MacKinnon and co-workers implied similar micellar defects to account for lipid-mediated voltage gating of neuronal potassium channels. The elastic and transient nature of micellar pores is consistent with the translocation of also CPPs that carry large, even giant, substrates. Sealed throughout without any content leakage, such pores can conceivably expand temporarily to match the diameter of the substrate and contract and self-heal once they have passed (Figure 16).

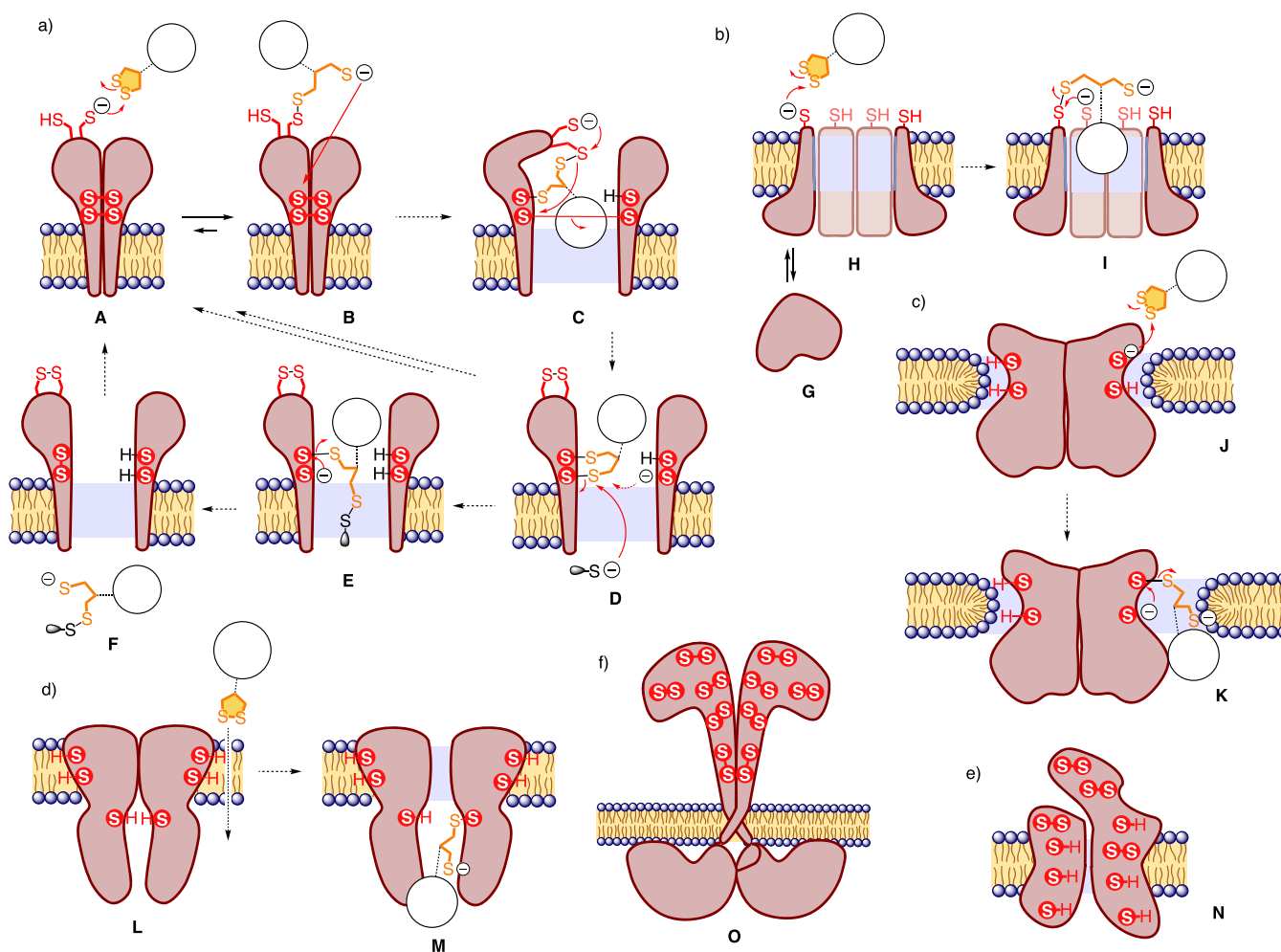


**Figure 17.** Hypothetical thiol-mediated uptake mechanisms with disulfide-network candidates covering (a) transferrin receptor (TFR), (b) chloride intracellular channel protein 1 (CLIC1), (c) Ca<sup>2+</sup>-activated scramblase (TMEM16F), (d) transient receptor potential cation channel (TRPA1), (e) voltage-gated calcium channel (Ca<sub>v</sub>1.1), and (f) epidermal growth factor receptor (EGFR).

For the remarkably efficient, endocytosis- and fusion-independent cytosolic delivery with CPDs and COCs, contributions from transient micellar pores offer a plausible explanation. Contrary to the repulsion-driven ion pairing<sup>165</sup> that binds CPPs to anionic membrane surfaces, micellar pore formation during thiol-mediated uptake would coincide with the unfolding of adaptive networks by dynamic covalent chalcogenide exchange chemistry and local protein denaturation, as described in the preceding chapters (Figure 16). Possible protein targets participating in these events will be briefly portrayed in the following.

### 5.7. Target Identification

While micellar pores may or may not contribute to direct translocation during thiol-mediated uptake, the cellular targets of dynamic covalent sulfur exchange most likely do. However, their involvement beyond dynamic covalent exchange remains to be determined, and their nature, with a few exceptions, remains to be identified.

Target identification for thiol-mediated uptake is complicated by the dynamic nature of the process. While proteomics analysis is, of course, possible,<sup>173</sup> it is difficult to tell if the detected proteins are really relevant for thiol-mediated uptake. The most reliable feedback can be obtained by suppression and overexpression of interesting candidates.<sup>173,50,139</sup> How-

ever, laborious suppression–overexpression approaches evaluating one target after the other cope poorly with the high number of possible targets. The most developed example for multiple targets in thiol-mediated uptake is the transferrin receptor (TFRC), identified top in proteomics analysis and validated by suppression–overexpression for AspA 5 but less relevant for ETP 25 (Figure 6).<sup>173</sup> These proteomics results and protein data bank analysis reveal an overwhelming number of possible targets for thiol-mediated uptake. In the following, a few short portraits of the most inspiring candidates are provided (Figure 17).

TFRC (Figure 17a), the transferrin receptor, is a highly abundant transmembrane protein on the cell surface. It enters cells by clathrin-mediated endocytosis after binding to the transferrin–iron complex and returns to the cell surface after releasing iron. Many drug delivery systems have been developed to profit from this system.<sup>174</sup> Various viruses, including SARS-CoV-2, also use TFRC binding for their entry into cells.<sup>175,176</sup>

Proteomics studies using fluorescently labeled AspA 5 identified TFRC as the top candidate to mediate its cellular uptake. Reduced uptake of AspA upon mutations of a pair of Cys 556/558 demonstrated their critical importance.<sup>173</sup> Thus, the first step of the thiol-mediated uptake through TFRC should be a ring-opening exchange between one of these

cysteine thiolates and a COC (Figures 17a, A, B and 9a). The resulting TFRC–chalcogenide conjugate **B** could enter the cell by endocytosis, but to reach the cytosol, the chalcogenide has to dissociate from TFRC and cross the membrane. The formed thiolate (or selenolate) might undergo further exchange reactions with disulfides near the membrane water interface stapling two TFRC units, which would require a significant protein conformational change (**B**, **C**). Cleavage of the two disulfide bonds could allow the two protein units to dissociate and expose space for the COC to slip through (**C**, **D**). The covalent bonds between TFRC and chalcogenides could be cleaved by reacting with an intracellular exchanger, e.g., glutathione (**D–F**), or with the thiols on the other TFRC unit (**D**, **A**) to release the chalcogenide inside of the cell and recover TFRC in the original state.

Contrary to AspA **5**, thiol-mediated uptake of ETP **25** is much less sensitive to TFRC knockdown (Figure 6).<sup>89</sup> This observation supports insights from inhibitor selectivity and proteomics that more than one pathway is available for thiol-mediated uptake (Figure 8).<sup>7</sup> siRNA–CPD polyplexes conjugated to transferrin have been shown to enter deep tissue by transcytosis, but contributions from dynamic covalent exchange chemistry have not been considered.<sup>60</sup>

CLIC1, the chloride intracellular channel protein 1, is a cytosolic protein that exists in both soluble (**G**) and membrane-bound forms (**H**, Figure 17b).<sup>177–179</sup> Conductance measurements show that soluble CLIC1 **G** added to one side (*cis*) of a bilayer membrane inserts spontaneously in the membrane and forms poorly selective anion channels **H**.<sup>180</sup> Importantly, the conductance can be regulated by the addition of thiol-reactive agents, such as *N*-ethylmaleimide (NEM), to the opposite side (*trans*) of the membrane. Thus, the reactive Cys24 is accessible to the aqueous medium at the other side of the membrane, which is, if extrapolated to *in vivo*, the extracellular side. The same Cys24 is also the critical residue for CLIC1's glutathione *S*-transferase like activity in the soluble form **G**.<sup>181</sup> Although the structure of the membrane-bound form **H** is not known, it is believed to consist of helix bundles forming barrel-stave like structure. The presence of different conductance levels implies that the number of monomer units and thus the channel diameter can vary.<sup>178</sup>

CLIC1 was one of the top five proteins identified by the proteomics study with AspA **5**.<sup>173</sup> The reaction of COCs with Cys24 of CLIC1 in the membrane-bound form **H**, followed by the disulfide exchange with another Cys24 of another monomer unit (**I**), might release COCs in the adaptable CLIC1 channels to pass through.

TMEM16F (Figure 17c), a Ca<sup>2+</sup>-activated scramblase, mediates bidirectional flip-flop of phospholipids in an energy-independent manner.<sup>182–184</sup> Upon activation, the hydrophilic micellar-type pores open within the protein to allow the translocation of hydrophilic lipid head groups across the hydrophobic core of the membrane (**J**). Its sensitivity to thiol-reactive agents is implied by its involvement in the formation of giant plasma membrane vesicles (GPMVs) by the action of NEM and paraformaldehyde.<sup>185</sup> Moreover, several cysteine residues are located in the transmembrane helices near the micellar hydrophilic pore. Thus, the reaction of these cysteines with COCs followed by its passage through micellar pores might be possible (**J**, **K**). TMEM16F arguably comes closest to the hypothesis combining micellar pores with adaptive sulfur networks, at best molecular walkers (Figures 9a and 16).

TRPA1 (Figure 17d), the transient receptor potential cation channel, also called the “wasabi receptor”, is activated by a wide variety of thiolate reactive electrophiles, including the wasabi and mustard component, allyl isocyanate, cinnamaldehyde, and the more electrophilic superspice **71** (Figures 17d and 13).<sup>152,186</sup> The binding sites Cys 415/422/622 are in the cytosol and thus not easily accessible to a hydrophilic COC.<sup>152</sup> However, other cysteine residues present within the transmembrane helices might contribute to the passage of COCs via thiolate–dichalcogenide exchange (**L**, **M**, Figure 17d).

Ca<sub>v</sub>1.1 (Figure 17e), a voltage-gated calcium channel, contains many cysteine residues in the transmembrane helices (**N**). Its redox sensitivity was shown by the oxidative (GSSG or DTNB) or reductive (GSH or DTT) treatment to result in the increase or decrease of the open probability of the ion channels, respectively.<sup>187</sup> Similar modulations of transport activities by thiol-reactive agents were also noted for a cystine/glutamate antiporter<sup>188</sup> and organic anion transporter.<sup>189</sup> These highly reactive cysteines are thus located near the transport pathways and might contribute to the thiol-mediated uptake in the manner similar to that of CLIC1.

EGFR (Figure 17f), the epidermal growth factor receptor, is a transmembrane receptor protein circulating between the plasma membrane and the endosomes, similarly to TFRC.<sup>190</sup> The extracellular part of this protein (**O**) is particularly rich in cysteine/cystine residues and is known to be targeted by dithiolanes and thiosulfonates.<sup>139,191</sup> In the elegant work of Castellano and co-workers, EGFR has been proposed to be the target of cyclic thiosulfonates similar to **6** (Figure 9d).<sup>139</sup> Cascade opening converting one exofacial thiol and one disulfide into one disulfide and one thiosulfonate bridge plus one new exofacial thiol has been suggested to ultimately account for antitumor activity. Crooke and co-workers have demonstrated that EGFR directly interacts with phosphorothioate antisense oligonucleotides **44** during their uptake into the cytosol and that EGFR suppression and overexpression reduce and enhance uptake via clathrin-mediated endocytosis (Figure 9b). Although the lack of cysteines in the transmembrane helices may (or may not) be incompatible with disulfide tracks for walking, this protein might capture COCs, pass them on to the other proteins to be transported across the membrane, or find other ways to mediate translocation.

Such roles can possibly be played by many other cysteine-rich proteins, such as integrins,<sup>192</sup> mucins,<sup>193</sup> or scavenger receptors. Scavenger receptor class B type 1 (SCARB1), for instance, is attractive because it is a membrane protein responsible for cholesteryl ester uptake, a proteomics target of AspA **5**,<sup>173</sup> and involved in the uptake of phosphorothioate RNA **44**<sup>49</sup> and hepatitis virus<sup>194</sup> (which is known to be thiol-mediated).<sup>195</sup>

PDIs (Figure 18), protein disulfide isomerases, are soluble thiol oxidoreductases of a thioredoxin superfamily. They locate mainly in the ER and assist the oxidative folding of nascent proteins. However, they are also found in the cytosol, in mitochondria, in nuclei, and on cell surfaces.<sup>196,197</sup> Extracellular PDIs associate to the cell surface through binding to the other surface-confined proteins, such as galectin-9, which in turn binds to glycosylated membrane proteins.<sup>198</sup> The cell surface PDIs are involved in, for example, cell adhesion, nitrosyl transfer, and viral entry.<sup>8,199</sup>

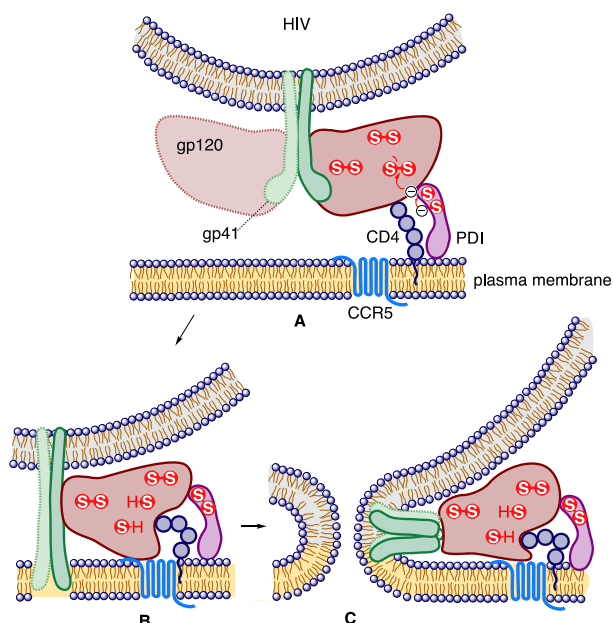


**Figure 18.** Thiol-mediated uptake of HIV:DTNB-inhibitable dynamic covalent disulfide exchange between PDI and gp120 (A, B) prepares for fusion (C).

### 5.8. Viral Uptake

As already outlined in the introduction, HIV entry has been one of the earliest observed examples of thiol-mediated uptake (Figure 2).<sup>1,8</sup> The developed mechanism suggests that HIV attaches to the cells by the binding of gp120 and CD4 (Figure 18, A). Then, PDI bound to CD4 reduces disulfides in gp120 to induce the conformational change needed to expose the N-terminus of gp41, which spontaneously inserts into the membrane (B) to prepare for fusion controlled by the popular helix bundle formation (C). This mechanism is supported by inhibition with Ellman's reagent **1** (Figure 2) and arsine oxides similar to Ehrlich's magic bullet **60** (Figure 12).<sup>8,146</sup>

By now, it is known that many other viruses use thiol-disulfide exchange to initiate cell entry, including Sindbis<sup>200,201</sup> and the LDV virus,<sup>202</sup> some coronaviruses,<sup>203–205</sup> murine leukemia virus,<sup>206,207</sup> baculovirus,<sup>208</sup> Newcastle disease,<sup>209</sup> or hepatitis.<sup>195,210</sup> With toxins, dynamic covalent exchange on cell surfaces (diphtheria)<sup>14,211,212</sup> is less common than enzymatic reduction after endocytosis (ricin,<sup>14,213</sup> cholera,<sup>214</sup> pseudomonas exotoxin,<sup>215</sup> and anthrax<sup>216</sup>). Many bacteria and parasites require thiols for attachment to mammalian cells.<sup>217–223</sup>

The involvement of thiol-mediated uptake in the entry of SARS-CoV-2 has received little support so far. The best established model is centered around the molecular recognition between the spike protein of the virus and ACE2, the angiotensin-converting enzyme 2.<sup>9,224,225</sup> The recognition can be followed by clathrin-dependent endocytosis, with the cathepsin cysteine proteases essential for endosomal escape. Alternatively, the serine protease TMPRSS2 on the cell surface can activate the spike/ACE2 complex for clathrin-independent membrane fusion. The understanding of these mechanisms is under constant evolution. The cell surface proteins neuropilin-1 and the serine protease furin have been added recently.<sup>226</sup> The most recent confirmation that the transferrin receptor is involved in SARS-CoV-2 entry<sup>176</sup> is particularly intriguing because it is a proteomics-confirmed target of thiol-mediated

uptake<sup>173</sup> and overexpressed on the blood–brain barrier endothelial cells for iron transport by transcytosis.<sup>60</sup>

Also very recently, we have identified inhibitors that are active against both thiol-mediated uptake and SARS-CoV-2 entry.<sup>7</sup> The best so far are several cyclic thiosulfonates **6**, better than the much discussed ebselens **42** (Figure 8). The future will tell if this is more than a coincidence. The same holds for TFRC as a common target,<sup>60,173,176</sup> EGFR as an interesting candidate,<sup>50,139</sup> and possibly also SCARB1<sup>173,194,195</sup> and other candidates outlined in section 5.7. Other targets have been proposed for all active compounds, including zinc fingers<sup>227</sup> and cysteine proteases<sup>129,130</sup> that are presumably not involved with cellular uptake, and multitarget mechanisms are quite likely.<sup>128</sup>

## 6. CONCLUSIONS

Thiol-mediated uptake is fascinating because it works so well in practice, while the modes of action are essentially unknown. Dynamic covalent chalcogenide exchange chemistry appears to account for both sides of the coin. In the spirit of a Perspective, we spend only a little time summarizing the many successful applications of thiol-mediated uptake in biology that have already been reviewed elsewhere.<sup>70,115–117,119</sup> Instead, we tried to map out the chemical space that enriches and complicates the elucidation of possible modes of action.

The result is a collection of classics in dynamic covalent chemistry, combining adaptive networks with templated polymerization, molecular walkers with micellar pores and affinity chromatography, and a gallery of membrane proteins as possible partners. The covered topics all relate to dynamic covalent processes, which means that they are hard to detect and characterize. This does not mean that they are absent or less significant. Quite the contrary, they all stand for translational supramolecular chemistry at its best, supporting the general expectation that focusing on different, underrecognized, perhaps elusive, and at best new ways to get into contact on the molecular level will ultimately allow us to tackle some of the more persistent challenges in science and society, here to unravel new ways to get into cells, and, perhaps, to stop viruses to do the same.

The relevance of most of this collection of classics in supramolecular chemistry for thiol-mediated uptake and the discovery of antivirals remain to be seen. Illustrating the breadth, complexity, and beauty of the topic, they are developed in this Perspective to outline inspirational possibilities that wait to be explored, with the objective to ultimately understand all the different expressions of thiol-mediated uptake, to understand how it really works.

## AUTHOR INFORMATION

### Corresponding Author

**Stefan Matile** – Department of Organic Chemistry, University of Geneva, 1211 Geneva, Switzerland; [orcid.org/0000-0002-8537-8349](https://orcid.org/0000-0002-8537-8349); Email: [stefan.matile@unige.ch](mailto:stefan.matile@unige.ch)

### Authors

**Quentin Laurent** – Department of Organic Chemistry, University of Geneva, 1211 Geneva, Switzerland

**Rémi Martinet** – Department of Organic Chemistry, University of Geneva, 1211 Geneva, Switzerland

**Bumhee Lim** – Department of Organic Chemistry, University of Geneva, 1211 Geneva, Switzerland

Anh-Tuan Pham – Department of Organic Chemistry,  
University of Geneva, 1211 Geneva, Switzerland

Takehiro Kato – Department of Organic Chemistry,  
University of Geneva, 1211 Geneva, Switzerland

Javier López-Andarias – Department of Organic Chemistry,  
University of Geneva, 1211 Geneva, Switzerland

Naomi Sakai – Department of Organic Chemistry, University  
of Geneva, 1211 Geneva, Switzerland; [orcid.org/0000-0002-9460-1944](https://orcid.org/0000-0002-9460-1944)

Complete contact information is available at:  
<https://pubs.acs.org/10.1021/jacsau.1c00128>

## Notes

The authors declare the following competing financial interest(s): A U.S. Patent Application has been filed covering the antiviral activity of cyclic thiosulfonates (No. 63/073,863).

## ACKNOWLEDGMENTS

We thank past and present co-workers and collaborators that contributed to research on this topic and the University of Geneva, the National Centre for Competence in Research (NCCR) in Chemical Biology, the NCCR Molecular Systems Engineering, and the Swiss NSF for financial support.

## REFERENCES

- (1) Feener, E. P.; Shen, W. C.; Ryser, H. J.-P. Cleavage of Disulfide Bonds in Endocytosed Macromolecules. A Processing Not Associated with Lysosomes or Endosomes. *J. Biol. Chem.* **1990**, *265*, 18780–18785.
- (2) Kichler, A.; Remy, J. S.; Boussif, O.; Frisch, B.; Boeckler, C.; Behr, J. P.; Schuber, F. Efficient Gene Delivery with Neutral Complexes of Lipospermine and Thiol-Reactive Phospholipids. *Biochem. Biophys. Res. Commun.* **1995**, *209*, 444–450.
- (3) Aubry, S.; Burlina, F.; Dupont, E.; Delaroche, D.; Joliot, A.; Lavielle, S.; Chassaing, G.; Sagan, S. Cell-Surface Thiols Affect Cell Entry of Disulfide-Conjugated Peptides. *FASEB J.* **2009**, *23*, 2956–2967.
- (4) Torres, A. G.; Gait, M. J. Exploiting Cell Surface Thiols to Enhance Cellular Uptake. *Trends Biotechnol.* **2012**, *30*, 185–190.
- (5) Gasparini, G.; Bang, E.-K.; Molinard, G.; Tulumello, D. V.; Ward, S.; Kelley, S. O.; Roux, A.; Sakai, N.; Matile, S. Cellular Uptake of Substrate-Initiated Cell-Penetrating Poly(disulfide)s. *J. Am. Chem. Soc.* **2014**, *136*, 6069–6074.
- (6) Gasparini, G.; Sargsyan, G.; Bang, E.-K.; Sakai, N.; Matile, S. Ring Tension Applied to Thiol-Mediated Cellular Uptake. *Angew. Chem., Int. Ed.* **2015**, *54*, 7328–7331.
- (7) Cheng, Y.; Pham, A.-T.; Kato, T.; Lim, B.; Moreau, D.; López-Andarias, J.; Zong, L.; Sakai, N.; Matile, S. Inhibitors of Thiol-Mediated Uptake. *Chem. Sci.* **2021**, *12*, 626–631.
- (8) Ryser, H. J.-P.; Flückiger, R. Keynote Review: Progress in Targeting HIV-1 Entry. *Drug Discovery Today* **2005**, *10*, 1085–1094.
- (9) Xiu, S.; Dick, A.; Ju, H.; Mirzaie, S.; Abdi, F.; Cocklin, S.; Zhan, P.; Liu, X. Inhibitors of SARS-CoV-2 Entry: Current and Future Opportunities. *J. Med. Chem.* **2020**, *63*, 12256–12274.
- (10) Li, J.; Nowak, P.; Otto, S. Dynamic Combinatorial Libraries: From Exploring Molecular Recognition to Systems Chemistry. *J. Am. Chem. Soc.* **2013**, *135*, 9222–9239.
- (11) Cougnon, F. B. L.; Sanders, J. K. M. Evolution of Dynamic Combinatorial Chemistry. *Acc. Chem. Res.* **2012**, *45*, 2211–2221.
- (12) Phan, N.-M.; Percástegui, E. G.; Johnson, D. W. Dynamic Covalent Chemistry as a Facile Route to Unusual Main-Group Thiolate Assemblies and Disulfide Hoops and Cages. *ChemPlusChem* **2020**, *85*, 1270–1282.
- (13) Liu, B.; Pappas, C. G.; Zangrando, E.; Demitri, N.; Chmielewski, P. J.; Otto, S. Complex Molecules That Fold Like Proteins Can Emerge Spontaneously. *J. Am. Chem. Soc.* **2019**, *141*, 1685–1689.
- (14) Ryser, H. J.-P.; Mandel, R.; Ghani, F. Cell Surface Sulfhydryls Are Required for the Cytotoxicity of Diphtheria Toxin but Not of Ricin in Chinese Hamster Ovary Cells. *J. Biol. Chem.* **1991**, *266*, 18439–18442.
- (15) Kichler, A.; Remy, J.-S.; Behr, J.-P.; Schuber, F. Targeted Transfection of Human Hepatoma Cells with a Combination of Lipospermine and Neo-Galactolipids. *J. Liposome Res.* **1995**, *5*, 735–745.
- (16) Saito, G.; Amidon, G. L.; Lee, K.-D. Enhanced Cytosolic Delivery of Plasmid DNA by a Sulfhydryl-Activatable Listeriolysin O/Protamine Conjugate Utilizing Cellular Reducing Potential. *Gene Ther.* **2003**, *10*, 72–83.
- (17) Jha, D.; Mishra, R.; Gottschalk, S.; Wiesmüller, K.-H.; Ugurbil, K.; Maier, M. E.; Engelmann, J. CyLoP-1: A Novel Cysteine-Rich Cell-Penetrating Peptide for Cytosolic Delivery of Cargoes. *Bioconjugate Chem.* **2011**, *22*, 319–328.
- (18) Digilio, G.; Menchise, V.; Gianolio, E.; Catanzaro, V.; Carrera, C.; Napolitano, R.; Fedeli, F.; Aime, S. Exofacial Protein Thiols as a Route for the Internalization of Gd(III)-Based Complexes for Magnetic Resonance Imaging Cell Labeling. *J. Med. Chem.* **2010**, *53*, 4877–4890.
- (19) Menchise, V.; Digilio, G.; Gianolio, E.; Cittadino, E.; Catanzaro, V.; Carrera, C.; Aime, S. In Vivo Labeling of B16 Melanoma Tumor Xenograft with a Thiol-Reactive Gadolinium Based MRI Contrast Agent. *Mol. Pharmaceutics* **2011**, *8*, 1750–1756.
- (20) Zhao, L.; Bai, F.; Chen, F.; Guo, M.; Gan, L.; Zhang, H.; Fang, J. A  $\beta$ -Allyl Carbamate Fluorescent Probe for Vicinal Dithiol Proteins. *Chem. Commun.* **2020**, *56*, 2857–2860.
- (21) Yi, M. C.; Khosla, C. Thiol–Disulfide Exchange Reactions in the Mammalian Extracellular Environment. *Annu. Rev. Chem. Biomol. Eng.* **2016**, *7*, 197–222.
- (22) Li, T.; Gao, W.; Liang, J.; Zha, M.; Chen, Y.; Zhao, Y.; Wu, C. Biscysteine-Bearing Peptide Probes To Reveal Extracellular Thiol–Disulfide Exchange Reactions Promoting Cellular Uptake. *Anal. Chem.* **2017**, *89*, 8501–8508.
- (23) Wang, Y.; Yang, X.-F.; Zhong, Y.; Gong, X.; Li, Z.; Li, H. Development of a Red Fluorescent Light-up Probe for Highly Selective and Sensitive Detection of Vicinal Dithiol-Containing Proteins in Living Cells. *Chem. Sci.* **2016**, *7*, 518–524.
- (24) Nitsche, C.; Mahawaththa, M. C.; Becker, W.; Huber, T.; Otting, G. Site-Selective Tagging of Proteins by Pnictogen-Mediated Self-Assembly. *Chem. Commun.* **2017**, *53*, 10894–10897.
- (25) Hu, G.; Jia, H.; Hou, Y.; Han, X.; Gan, L.; Si, J.; Cho, D.-H.; Zhang, H.; Fang, J. Decrease of Protein Vicinal Dithiols in Parkinsonism Disclosed by a Monoarsenical Fluorescent Probe. *Anal. Chem.* **2020**, *92*, 4371–4378.
- (26) Gao, W.; Li, T.; Wang, J.; Zhao, Y.; Wu, C. Thioether-Bonded Fluorescent Probes for Deciphering Thiol-Mediated Exchange Reactions on the Cell Surface. *Anal. Chem.* **2017**, *89*, 937–944.
- (27) Huang, C.; Yin, Q.; Zhu, W.; Yang, Y.; Wang, X.; Qian, X.; Xu, Y. Highly Selective Fluorescent Probe for Vicinal-Dithiol-Containing Proteins and in Situ Imaging in Living Cells. *Angew. Chem., Int. Ed.* **2011**, *50*, 7551–7556.
- (28) Huang, C.; Jia, T.; Tang, M.; Yin, Q.; Zhu, W.; Zhang, C.; Yang, Y.; Jia, N.; Xu, Y.; Qian, X. Selective and Ratiometric Fluorescent Trapping and Quantification of Protein Vicinal Dithiols and in Situ Dynamic Tracing in Living Cells. *J. Am. Chem. Soc.* **2014**, *136*, 14237–14244.
- (29) Yang, Z.; Kang, D. H.; Lee, H.; Shin, J.; Yan, W.; Rathore, B.; Kim, H.-R.; Kim, S. J.; Singh, H.; Liu, L.; Qu, J.; Kang, C.; Kim, J. S. A Fluorescent Probe for Stimulated Emission Depletion Super-Resolution Imaging of Vicinal-Dithiol-Proteins on Mitochondrial Membrane. *Bioconjugate Chem.* **2018**, *29*, 1446–1453.
- (30) Brülisauer, L.; Kathriner, N.; Prenrecaj, M.; Gauthier, M. A.; Leroux, J.-C. Tracking the Bioreduction of Disulfide-Containing Cationic Dendrimers. *Angew. Chem., Int. Ed.* **2012**, *51*, 12454–12458.

- (31) Arafles, J. V. V.; Hirose, H.; Hirai, Y.; Kuriyama, M.; Sakyamah, M. M.; Nomura, W.; Sonomura, K.; Imanishi, M.; Otake, A.; Tamamura, H.; Futaki, S. Discovery of a Macropinocytosis-Inducing Peptide Potentiated by Medium-Mediated Intramolecular Disulfide Formation. *Angew. Chem., Int. Ed.* **2021**, DOI: 10.1002/anie.202016754.
- (32) Bode, S. A.; Wallbrecher, R.; Brock, R.; van Hest, J. C. M.; Löwik, D. W. P. M. Activation of Cell-Penetrating Peptides by Disulfide Bridge Formation of Truncated Precursors. *Chem. Commun.* **2014**, *50*, 415–417.
- (33) Oberhauser, B.; Wagner, E. Effective Incorporation of 2'-O-Methyl-Oligoribonucleotides into Liposomes and Enhanced Cell Association through Modification with Thiocholesterol. *Nucleic Acids Res.* **1992**, *20*, 533–538.
- (34) Weller, K.; Lauber, S.; Lerch, M.; Renaud, A.; Merkle, H. P.; Zerbe, O. Biophysical and Biological Studies of End-Group-Modified Derivatives of Pep-1. *Biochemistry* **2005**, *44*, 15799–15811.
- (35) Fang, S.; Fan, T.; Fu, H.-W.; Chen, C.-J.; Hwang, C.-S.; Hung, T.-J.; Lin, L.-Y.; Chang, M. D.-T. A Novel Cell-Penetrating Peptide Derived from Human Eosinophil Cationic Protein. *PLoS One* **2013**, *8*, e57318.
- (36) D'Souza, C.; Troeira Henriques, S.; Wang, C. K.; Craik, D. J. Structural Parameters Modulating the Cellular Uptake of Disulfide-Rich Cyclic Cell-Penetrating Peptides: MCoTI-II and SFTI-1. *Eur. J. Med. Chem.* **2014**, *88*, 10–18.
- (37) Shirazi, A. N.; El-Sayed, N. S.; Mandal, D.; Tiwari, R. K.; Tavakoli, K.; Etesham, M.; Parang, K. Cysteine and Arginine-Rich Peptides as Molecular Carriers. *Bioorg. Med. Chem. Lett.* **2016**, *26*, 656–661.
- (38) Kam, A.; Loo, S.; Fan, J.-S.; Sze, S. K.; Yang, D.; Tam, J. P. Roseltide RT7 Is a Disulfide-Rich, Anionic, and Cell-Penetrating Peptide That Inhibits Proteasomal Degradation. *J. Biol. Chem.* **2019**, *294*, 19604–19615.
- (39) Theodore, L.; Derossi, D.; Chassaing, G.; Llirbat, B.; Kubas, M.; Jordan, P.; Chneiweiss, H.; Godement, P.; Prochiantz, A. Intraneuronal Delivery of Protein Kinase C Pseudosubstrate Leads to Growth Cone Collapse. *J. Neurosci.* **1995**, *15*, 7158–7167.
- (40) Chaloin, L.; Vidal, P.; Lory, P.; Méry, J.; Lautredou, N.; Divita, G.; Heitz, F. Design of Carrier Peptide-Oligonucleotide Conjugates with Rapid Membrane Translocation and Nuclear Localization Properties. *Biochem. Biophys. Res. Commun.* **1998**, *243*, 601–608.
- (41) Pooga, M.; Soomets, U.; Hällbrink, M.; Valkna, A.; Saar, K.; Rezaei, K.; Kahl, U.; Hao, J.-X.; Xu, X.-J.; Wiesenfeld-Hallin, Z.; Hökfelt, T.; Bartfai, T.; Langel, Ü. Cell Penetrating PNA Constructs Regulate Galanin Receptor Levels and Modify Pain Transmission in Vivo. *Nat. Biotechnol.* **1998**, *16*, 857–861.
- (42) Astriab-Fisher, A.; Sergueev, D. S.; Fisher, M.; Ramsay Shaw, B.; Juliano, R. L. Antisense Inhibition of P-Glycoprotein Expression Using Peptide–Oligonucleotide Conjugates. *Biochem. Pharmacol.* **2000**, *60*, 83–90.
- (43) Fujimoto, K.; Hosotani, R.; Miyamoto, Y.; Doi, R.; Koshiha, T.; Otake, A.; Fujii, N.; Beauchamp, R. D.; Imamura, M. Inhibition of PRb Phosphorylation and Cell Cycle Progression by an Antennapedia-P16INK4A Fusion Peptide in Pancreatic Cancer Cells. *Cancer Lett.* **2000**, *159*, 151–158.
- (44) Lei, E. K.; Kelley, S. O. Delivery and Release of Small-Molecule Probes in Mitochondria Using Traceless Linkers. *J. Am. Chem. Soc.* **2017**, *139*, 9455–9458.
- (45) Schneider, A. F. L.; Wallabregue, A. L. D.; Franz, L.; Hackenberger, C. P. R. Targeted Subcellular Protein Delivery Using Cleavable Cyclic Cell-Penetrating Peptides. *Bioconjugate Chem.* **2019**, *30*, 400–404.
- (46) Tombling, B. J.; Wang, C. K.; Craik, D. J. EGF-like and Other Disulfide-Rich Microdomains as Therapeutic Scaffolds. *Angew. Chem., Int. Ed.* **2020**, *59*, 11218–11232.
- (47) Fretz, M. M.; Penning, N. A.; Al-Taei, S.; Futaki, S.; Takeuchi, T.; Nakase, I.; Storm, G.; Jones, A. T. Temperature-, Concentration- and Cholesterol-Dependent Translocation of L- and D-Octa-Arginine across the Plasma and Nuclear Membrane of CD34+ Leukaemia Cells. *Biochem. J.* **2007**, *403*, 335–342.
- (48) Castanotto, D.; Lin, M.; Kowolik, C.; Wang, L.; Ren, X.-Q.; Soifer, H. S.; Koch, T.; Hansen, B. R.; Oerum, H.; Armstrong, B.; Wang, Z.; Bauer, P.; Rossi, J.; Stein, C. A. A Cytoplasmic Pathway for Gapmer Antisense Oligonucleotide-Mediated Gene Silencing in Mammalian Cells. *Nucleic Acids Res.* **2015**, *43*, 9350–9361.
- (49) Crooke, S. T.; Seth, P. P.; Vickers, T. A.; Liang, X. The Interaction of Phosphorothioate-Containing RNA Targeted Drugs with Proteins Is a Critical Determinant of the Therapeutic Effects of These Agents. *J. Am. Chem. Soc.* **2020**, *142*, 14754–14771.
- (50) Wang, S.; Allen, N.; Vickers, T. A.; Revenko, A. S.; Sun, H.; Liang, X.-H.; Crooke, S. T. Cellular Uptake Mediated by Epidermal Growth Factor Receptor Facilitates the Intracellular Activity of Phosphorothioate-Modified Antisense Oligonucleotides. *Nucleic Acids Res.* **2018**, *46*, 3579–3594.
- (51) Tjin, C. C.; Otley, K. D.; Baguley, T. D.; Kurup, P.; Xu, J.; Nairn, A. C.; Lombroso, P. J.; Ellman, J. A. Glutathione-Responsive Selenosulfide Prodrugs as a Platform Strategy for Potent and Selective Mechanism-Based Inhibition of Protein Tyrosine Phosphatases. *ACS Cent. Sci.* **2017**, *3*, 1322–1328.
- (52) Oupický, D.; Li, J. Bioreducible Polycations in Nucleic Acid Delivery: Past, Present, and Future Trends. *Macromol. Biosci.* **2014**, *14*, 908–922.
- (53) Lin, C.; Engbersen, J. F. The Role of the Disulfide Group in Disulfide-Based Polymeric Gene Carriers. *Expert Opin. Drug Delivery* **2009**, *6*, 421–439.
- (54) Kim, T.; Kim, S. W. Bioreducible Polymers for Gene Delivery. *React. Funct. Polym.* **2011**, *71*, 344–349.
- (55) Son, S.; Namgung, R.; Kim, J.; Singha, K.; Kim, W. J. Bioreducible Polymers for Gene Silencing and Delivery. *Acc. Chem. Res.* **2012**, *45*, 1100–1112.
- (56) Zeng, H.; Little, H. C.; Tiambeng, T. N.; Williams, G. A.; Guan, Z. Multifunctional Dendronized Peptide Polymer Platform for Safe and Effective siRNA Delivery. *J. Am. Chem. Soc.* **2013**, *135*, 4962–4965.
- (57) Drake, C. R.; Aissaoui, A.; Argyros, O.; Thanou, M.; Steinke, J. H. G.; Miller, A. D. Examination of the Effect of Increasing the Number of Intra-Disulfide Amino Functional Groups on the Performance of Small Molecule Cyclic Polyamine Disulfide Vectors. *J. Controlled Release* **2013**, *171*, 81–90.
- (58) Balakirev, M.; Schoehn, G.; Chroboczek, J. Lipic Acid-Derived Amphiphiles for Redox-Controlled DNA Delivery. *Chem. Biol.* **2000**, *7*, 813–819.
- (59) Hashim, P. K.; Okuro, K.; Sasaki, S.; Hoashi, Y.; Aida, T. Reductively Cleavable Nanocaplets for siRNA Delivery by Template-Assisted Oxidative Polymerization. *J. Am. Chem. Soc.* **2015**, *137*, 15608–15611.
- (60) Kohata, A.; Hashim, P. K.; Okuro, K.; Aida, T. Transferrin-Appended Nanocaplet for Transcellular siRNA Delivery into Deep Tissues. *J. Am. Chem. Soc.* **2019**, *141*, 2862–2866.
- (61) Sakai, N.; Matile, S. Anion-Mediated Transfer of Polyarginine across Liquid and Bilayer Membranes. *J. Am. Chem. Soc.* **2003**, *125*, 14348–14356.
- (62) Sakai, N.; Lista, M.; Kel, O.; Sakurai, S.; Emery, D.; Mareda, J.; Vauthey, E.; Matile, S. Self-Organizing Surface-Initiated Polymerization: Facile Access to Complex Functional Systems. *J. Am. Chem. Soc.* **2011**, *133*, 15224–15227.
- (63) Lista, M.; Areephong, J.; Sakai, N.; Matile, S. Lateral Self-Sorting on Surfaces: A Practical Approach to Double-Channel Photosystems. *J. Am. Chem. Soc.* **2011**, *133*, 15228–15231.
- (64) Sakai, N.; Matile, S. Stack Exchange Strategies for the Synthesis of Covalent Double-Channel Photosystems by Self-Organizing Surface-Initiated Polymerization. *J. Am. Chem. Soc.* **2011**, *133*, 18542–18545.
- (65) Sakai, N.; Sisson, A. L.; Bürgi, T.; Matile, S. Zipper Assembly of Photoactive Rigid-Rod Naphthalenediimide  $\pi$ -Stack Architectures on Gold Nanoparticles and Gold Electrodes. *J. Am. Chem. Soc.* **2007**, *129*, 15758–15759.

- (66) Bang, E.-K.; Gasparini, G.; Molinard, G.; Roux, A.; Sakai, N.; Matile, S. Substrate-Initiated Synthesis of Cell-Penetrating Poly(disulfide)s. *J. Am. Chem. Soc.* **2013**, *135*, 2088–2091.
- (67) Laurent, Q.; Sakai, N.; Matile, S. The Opening of 1,2-Dithiolanes and 1,2-Diselenolanes: Regioselectivity, Rearrangements, and Consequences for Poly(disulfide)s, Cellular Uptake and Pyruvate Dehydrogenase Complexes. *Helv. Chim. Acta* **2019**, *102*, e1800209.
- (68) Pulcu, G. S.; Galenkamp, N. S.; Qing, Y.; Gasparini, G.; Mikhailova, E.; Matile, S.; Bayley, H. Single-Molecule Kinetics of Growth and Degradation of Cell-Penetrating Poly(disulfide)s. *J. Am. Chem. Soc.* **2019**, *141*, 12444–12447.
- (69) Morelli, P.; Martin-Benlloch, X.; Tessier, R.; Waser, J.; Sakai, N.; Matile, S. Ethynyl Benziodoxolones: Functional Terminators for Cell-Penetrating Poly(disulfide)s. *Polym. Chem.* **2016**, *7*, 3465–3470.
- (70) Du, S.; Liew, S. S.; Li, L.; Yao, S. Q. Bypassing Endocytosis: Direct Cytosolic Delivery of Proteins. *J. Am. Chem. Soc.* **2018**, *140*, 15986–15996.
- (71) Yuan, P.; Mao, X.; Chong, K. C.; Fu, J.; Pan, S.; Wu, S.; Yu, C.; Yao, S. Q. Simultaneous Imaging of Endogenous Survivin mRNA and On-Demand Drug Release in Live Cells by Using a Mesoporous Silica Nanoquencher. *Small* **2017**, *13*, 1700569.
- (72) Mao, X.; Yuan, P.; Yu, C.; Li, L.; Yao, S. Q. Nanoquencher-Based Selective Imaging of Protein Glutathionylation in Live Mammalian Cells. *Angew. Chem., Int. Ed.* **2018**, *57*, 10257–10262.
- (73) Yuan, P.; Mao, X.; Wu, X.; Liew, S. S.; Li, L.; Yao, S. Q. Mitochondria-Targeting, Intracellular Delivery of Native Proteins Using Biodegradable Silica Nanoparticles. *Angew. Chem., Int. Ed.* **2019**, *58*, 7657–7661.
- (74) Fu, J.; Yu, C.; Li, L.; Yao, S. Q. Intracellular Delivery of Functional Proteins and Native Drugs by Cell-Penetrating Poly(disulfide)s. *J. Am. Chem. Soc.* **2015**, *137*, 12153–12160.
- (75) Yuan, P.; Zhang, H.; Qian, L.; Mao, X.; Du, S.; Yu, C.; Peng, B.; Yao, S. Q. Intracellular Delivery of Functional Native Antibodies under Hypoxic Conditions by Using a Biodegradable Silica Nanoquencher. *Angew. Chem., Int. Ed.* **2017**, *56*, 12481–12485.
- (76) Yu, C.; Qian, L.; Ge, J.; Fu, J.; Yuan, P.; Yao, S. C. L.; Yao, S. Q. Cell-Penetrating Poly(disulfide) Assisted Intracellular Delivery of Mesoporous Silica Nanoparticles for Inhibition of miR-21 Function and Detection of Subsequent Therapeutic Effects. *Angew. Chem., Int. Ed.* **2016**, *55*, 9272–9276.
- (77) Qian, L.; Fu, J.; Yuan, P.; Du, S.; Huang, W.; Li, L.; Yao, S. Q. Intracellular Delivery of Native Proteins Facilitated by Cell-Penetrating Poly(disulfide)s. *Angew. Chem., Int. Ed.* **2018**, *57*, 1532–1536.
- (78) Liu, Y.; Jia, Y.; Wu, Q.; Moore, J. S. Architecture-Controlled Ring-Opening Polymerization for Dynamic Covalent Poly(disulfide)s. *J. Am. Chem. Soc.* **2019**, *141*, 17075–17080.
- (79) Lu, J.; Wang, H.; Tian, Z.; Hou, Y.; Lu, H. Cryopolymerization of 1,2-Dithiolanes for the Facile and Reversible Grafting-from Synthesis of Protein–Polydisulfide Conjugates. *J. Am. Chem. Soc.* **2020**, *142*, 1217–1221.
- (80) Okamoto, Y.; Kojima, R.; Schwizer, F.; Bartolami, E.; Heinisch, T.; Matile, S.; Fussenegger, M.; Ward, T. R. A Cell-Penetrating Artificial Metalloenzyme Regulates a Gene Switch in a Designer Mammalian Cell. *Nat. Commun.* **2018**, *9*, 1943.
- (81) Derivery, E.; Bartolami, E.; Matile, S.; Gonzalez-Gaitan, M. Efficient Delivery of Quantum Dots into the Cytosol of Cells Using Cell-Penetrating Poly(disulfide)s. *J. Am. Chem. Soc.* **2017**, *139*, 10172–10175.
- (82) Yuan, P.; Mao, X.; Wu, X.; Liew, S. S.; Li, L.; Yao, S. Q. Mitochondria-Targeting, Intracellular Delivery of Native Proteins Using Biodegradable Silica Nanoparticles. *Angew. Chem., Int. Ed.* **2019**, *58*, 7657–7661.
- (83) Zhou, J.; Sun, L.; Wang, L.; Liu, Y.; Li, J.; Li, J.; Li, J.; Yang, H. Self-Assembled and Size-Controllable Oligonucleotide Nanospheres for Effective Antisense Gene Delivery through an Endocytosis-Independent Pathway. *Angew. Chem., Int. Ed.* **2019**, *58*, 5236–5240.
- (84) Clauss, A. D.; Nelsen, S. F.; Ayoub, M.; Moore, J. W.; Landis, C. R.; Weinholt, F. Rabbit-Ears Hybrids, VSEPR Sterics, and Other Orbital Anachronisms. *Chem. Educ. Res. Pract.* **2014**, *15*, 417–434.
- (85) Hiberty, P. C.; Braïda, B. Pleading for a Dual Molecular-Orbital/Valence-Bond Culture. *Angew. Chem., Int. Ed.* **2018**, *57*, 5994–6002.
- (86) Burns, J. A.; Whitesides, G. M. Predicting the Stability of Cyclic Disulfides by Molecular Modeling: Effective Concentrations in Thiol-Disulfide Interchange and the Design of Strongly Reducing Dithiols. *J. Am. Chem. Soc.* **1990**, *112*, 6296–6303.
- (87) Chuard, N.; Poblador-Bahamonde, A. I.; Zong, L.; Bartolami, E.; Hildebrandt, J.; Weigand, W.; Sakai, N.; Matile, S. Diselenolane-Mediated Cellular Uptake. *Chem. Sci.* **2018**, *9*, 1860–1866.
- (88) Kilgore, H. R.; Olsson, C. R.; D'Angelo, K. A.; Movassaghi, M.; Raines, R. T.  $n \rightarrow \pi^*$  Interactions Modulate the Disulfide Reduction Potential of Epidithiodiketopiperazines. *J. Am. Chem. Soc.* **2020**, *142*, 15107–15115.
- (89) Zong, L.; Bartolami, E.; Abegg, D.; Adibekian, A.; Sakai, N.; Matile, S. Epidithiodiketopiperazines: Strain-Promoted Thiol-Mediated Cellular Uptake at the Highest Tension. *ACS Cent. Sci.* **2017**, *3*, 449–453.
- (90) Cheng, Y.; Zong, L.; López-Andarias, J.; Bartolami, E.; Okamoto, Y.; Ward, T. R.; Sakai, N.; Matile, S. Cell-Penetrating Dynamic-Covalent Benzopolysulfane Networks. *Angew. Chem., Int. Ed.* **2019**, *58*, 9522–9526.
- (91) Jiang, C.-S.; Müller, W. E. G.; Schröder, H. C.; Guo, Y.-W. Disulfide- and Multisulfide-Containing Metabolites from Marine Organisms. *Chem. Rev.* **2012**, *112*, 2179–2207.
- (92) Kim, J.; Movassaghi, M. Biogenetically-Inspired Total Synthesis of Epidithiodiketopiperazines and Related Alkaloids. *Acc. Chem. Res.* **2015**, *48*, 1159–1171.
- (93) McDougall, J. K. Antiviral Action of Gliotoxin. *Arch. Virol.* **1969**, *27*, 255–267.
- (94) Steudel, R. The Chemistry of Organic Polysulfanes R–Sn–R ( $n > 2$ ). *Chem. Rev.* **2002**, *102*, 3905–3946.
- (95) Mahendran, A.; Vuong, A.; Aebischer, D.; Gong, Y.; Bittman, R.; Arthur, G.; Kawamura, A.; Greer, A. Synthesis, Characterization, Mechanism of Decomposition, and Antiproliferative Activity of a Class of PEGylated Benzopolysulfanes Structurally Similar to the Natural Product Varacin. *J. Org. Chem.* **2010**, *75*, 5549–5557.
- (96) Behar, V.; Danishefsky, S. J. Total Synthesis of the Novel Benzopentathiepin Varacinium Trifluoroacetate: The Viability of “Varacin-Free Base. *J. Am. Chem. Soc.* **1993**, *115*, 7017–7018.
- (97) Xu, J.; Chatterjee, M.; Baguley, T. D.; Brouillette, J.; Kurup, P.; Ghosh, D.; Kanyo, J.; Zhang, Y.; Seyb, K.; Ononenyi, C.; Foscue, E.; Anderson, G. M.; Gresack, J.; Cuny, G. D.; Glicksman, M. A.; Greengard, P.; Lam, T. T.; Tautz, L.; Nairn, A. C.; Ellman, J. A.; Lombroso, P. J. Inhibitor of the Tyrosine Phosphatase STEP Reverses Cognitive Deficits in a Mouse Model of Alzheimer's Disease. *PLoS Biol.* **2014**, *12*, e1001923.
- (98) López-Andarias, J.; Saabach, J.; Moreau, D.; Cheng, Y.; Derivery, E.; Laurent, Q.; González-Gaitán, M.; Winssinger, N.; Sakai, N.; Matile, S. Cell-Penetrating Streptavidin: A General Tool for Bifunctional Delivery with Spatiotemporal Control, Mediated by Transport Systems Such as Adaptive Benzopolysulfane Networks. *J. Am. Chem. Soc.* **2020**, *142*, 4784–4792.
- (99) Kishore, R.; Balaram, P. Stabilization of  $\gamma$ -Turn Conformations in Peptides by Disulfide Bridging. *Biopolymers* **1985**, *24*, 2041–2043.
- (100) Derewenda, U.; Boczek, T.; Gorres, K. L.; Yu, M.; Hung, L.; Cooper, D.; Joachimiak, A.; Raines, R. T.; Derewenda, Z. S. Structure and Function of Bacillus Subtilis YphP, a Prokaryotic Disulfide Isomerase with a CXC Catalytic Motif. *Biochemistry* **2009**, *48*, 8664–8671.
- (101) Schmidt, B.; Lindman, S.; Tong, W.; Lindeberg, G.; Gogoll, A.; Lai, Z.; Thörnwall, M.; Synnergren, B.; Nilsson, A.; Welch, C. J.; Sohtell, M.; Westerlund, C.; Nyberg, F.; Karlén, A.; Hallberg, A. Design, Synthesis, and Biological Activities of Four Angiotensin II Receptor Ligands with  $\gamma$ -Turn Mimetics Replacing Amino Acid Residues 3–5. *J. Med. Chem.* **1997**, *40*, 903–919.



- (102) Meng, X.; Li, T.; Zhao, Y.; Wu, C. CXC-Mediated Cellular Uptake of Mini-proteins: Forsaking “Arginine Magic.” *ACS Chem. Biol.* **2018**, *13*, 3078–3086.
- (103) Saneyoshi, H.; Ohta, T.; Hiyoshi, Y.; Saneyoshi, T.; Ono, A. Design, Synthesis, and Cellular Uptake of Oligonucleotides Bearing Glutathione-Labile Protecting Groups. *Org. Lett.* **2019**, *21*, 862–866.
- (104) Shu, Z.; Tanaka, I.; Ota, A.; Fushihara, D.; Abe, N.; Kawaguchi, S.; Nakamoto, K.; Tomoike, F.; Tada, S.; Ito, Y.; Kimura, Y.; Abe, H. Disulfide-Unit Conjugation Enables Ultrafast Cytosolic Internalization of Antisense DNA and siRNA. *Angew. Chem., Int. Ed.* **2019**, *58*, 6611–6615.
- (105) Shu, Z.; Ota, A.; Takayama, Y.; Katsurada, Y.; Kusamori, K.; Abe, N.; Nakamoto, K.; Tomoike, F.; Tada, S.; Ito, Y.; Nishikawa, M.; Kimura, Y.; Abe, H. Intracellular Delivery of Antisense DNA and siRNA with Amino Groups Masked with Disulfide Units. *Chem. Pharm. Bull.* **2020**, *68*, 129–132.
- (106) Martinent, R.; Du, D.; López-Andarias, J.; Sakai, N.; Matile, S. Oligomers of Cyclic Oligochalcogenides for Enhanced Cellular Uptake. *ChemBioChem* **2021**, *22*, 253–259.
- (107) Tirla, A.; Rivera-Fuentes, P. Peptide Targeting of an Intracellular Receptor of the Secretory Pathway. *Biochemistry* **2019**, *58*, 1184–1187.
- (108) Zhang, L.; Duan, D.; Liu, Y.; Ge, C.; Cui, X.; Sun, J.; Fang, J. Highly Selective Off–On Fluorescent Probe for Imaging Thioredoxin Reductase in Living Cells. *J. Am. Chem. Soc.* **2014**, *136*, 226–233.
- (109) Li, X.; Hou, Y.; Meng, X.; Ge, C.; Ma, H.; Li, J.; Fang, J. Selective Activation of a Prodrug by Thioredoxin Reductase Providing a Strategy to Target Cancer Cells. *Angew. Chem., Int. Ed.* **2018**, *57*, 6141–6145.
- (110) Li, X.; Hou, Y.; Zhao, J.; Li, J.; Wang, S.; Fang, J. Combination of Chemotherapy and Oxidative Stress to Enhance Cancer Cell Apoptosis. *Chem. Sci.* **2020**, *11*, 3215–3222.
- (111) Felber, J.; Poczka, L.; Busker, S.; Theisen, U.; Zeisel, L.; Maier, M. S.; Loy, K.; Brandstädter, C.; Scholzen, K.; Becker, K.; Arnér, E.; Ahlfeld, J.; Thorn-Seshold, O. Cyclic 5-Membered Disulfides Are Not Selective Substrates of Thioredoxin Reductase, but Are Opened Nonspecifically by Thiols. *ChemRxiv* **2020**, DOI: 10.26434/chemrxiv.13483155.v1.
- (112) Bartolami, E.; Basagiannis, D.; Zong, L.; Martinent, R.; Okamoto, Y.; Laurent, Q.; Ward, T. R.; Gonzalez-Gaitan, M.; Sakai, N.; Matile, S. Diselenolane-Mediated Cellular Uptake: Efficient Cytosolic Delivery of Probes, Peptides, Proteins, Artificial Metalloenzymes and Protein-Coated Quantum Dots. *Chem. - Eur. J.* **2019**, *25*, 4047–4051.
- (113) Chuard, N.; Gasparini, G.; Moreau, D.; Lörcher, S.; Palivan, C.; Meier, W.; Sakai, N.; Matile, S. Strain-Promoted Thiol-Mediated Cellular Uptake of Giant Substrates: Liposomes and Polymersomes. *Angew. Chem., Int. Ed.* **2017**, *56*, 2947–2950.
- (114) Ulrich, S. Growing Prospects of Dynamic Covalent Chemistry in Delivery Applications. *Acc. Chem. Res.* **2019**, *52*, 510–519.
- (115) Zhou, J.; Shao, Z.; Liu, J.; Duan, Q.; Wang, X.; Li, J.; Yang, H. From Endocytosis to Nonendocytosis: The Emerging Era of Gene Delivery. *ACS Appl. Bio Mater.* **2020**, *3*, 2686–2701.
- (116) Qin, X.; Yu, C.; Wei, J.; Li, L.; Zhang, C.; Wu, Q.; Liu, J.; Yao, S. Q.; Huang, W. Rational Design of Nanocarriers for Intracellular Protein Delivery. *Adv. Mater.* **2019**, *31*, 1902791.
- (117) Zhang, R.; Qin, X.; Kong, F.; Chen, P.; Pan, G. Improving Cellular Uptake of Therapeutic Entities through Interaction with Components of Cell Membrane. *Drug Delivery* **2019**, *26*, 328–342.
- (118) Zhang, Y.; Qi, Y.; Ulrich, S.; Barboiu, M.; Ramström, O. Dynamic Covalent Polymers for Biomedical Applications. *Mater. Chem. Front.* **2020**, *4*, 489–506.
- (119) Gui, L.; Zhang, X.-H.; Qiao, Z.-Y.; Wang, H. Cell-Penetrating Peptides and Polymers for Improved Drug Delivery. *ChemNanoMat* **2020**, *6*, 1138–1148.
- (120) Abegg, D.; Frei, R.; Cerato, L.; Prasad Hari, D.; Wang, C.; Wasser, J.; Adibekian, A. Proteome-Wide Profiling of Targets of Cysteine Reactive Small Molecules by Using Ethynyl Benziodoxolone Reagents. *Angew. Chem., Int. Ed.* **2015**, *54*, 10852–10857.
- (121) Tokunaga, K.; Sato, M.; Kuwata, K.; Miura, C.; Fuchida, H.; Matsunaga, N.; Koyanagi, S.; Ohdo, S.; Shindo, N.; Ojida, A. Bicyclobutane Carboxylic Amide as a Cysteine-Directed Strained Electrophile for Selective Targeting of Proteins. *J. Am. Chem. Soc.* **2020**, *142*, 18522–18531.
- (122) Litwin, K.; Crowley, V. M.; Suci, R. M.; Boger, D. L.; Cravatt, B. F. Chemical Proteomic Identification of Functional Cysteines with Atypical Electrophile Reactivities. *Tetrahedron Lett.* **2021**, *67*, 152861.
- (123) Donoghue, N.; Hogg, P. J. Characterization of Redox-Active Proteins on Cell Surface. *Methods Enzymol.* **2002**, *348*, 76–86.
- (124) Münchberg, U.; Anwar, A.; Mecklenburg, S.; Jacob, C. Polysulfides as Biologically Active Ingredients of Garlic. *Org. Biomol. Chem.* **2007**, *5*, 1505–1518.
- (125) Shojai, T. M.; Langeroudi, A. G.; Karimi, V.; Barin, A.; Sadri, N. The Effect of Allium Sativum (Garlic) Extract on Infectious Bronchitis Virus in Specific Pathogen Free Embryonic Egg. *Avicenna J. Phytomed.* **2016**, *6*, 458–267.
- (126) Motiwala, H. F.; Kuo, Y.-H.; Stinger, B. L.; Palfey, B. A.; Martin, B. R. Tunable Heteroaromatic Sulfones Enhance In-Cell Cysteine Profiling. *J. Am. Chem. Soc.* **2020**, *142*, 1801–1810.
- (127) Jin, Z.; Du, X.; Xu, Y.; Deng, Y.; Liu, M.; Zhao, Y.; Zhang, B.; Li, X.; Zhang, L.; Peng, C.; Duan, Y.; Yu, J.; Wang, L.; Yang, K.; Liu, F.; Jiang, R.; Yang, X.; You, T.; Liu, X.; Yang, X.; Bai, F.; Liu, H.; Liu, X.; Guddat, L. W.; Xu, W.; Xiao, G.; Qin, C.; Shi, Z.; Jiang, H.; Rao, Z.; Yang, H. Structure of Mpro from SARS-CoV-2 and Discovery of Its Inhibitors. *Nature* **2020**, *582*, 289–293.
- (128) Sargsyan, K.; Lin, C.-C.; Chen, T.; Grauffel, C.; Chen, Y.-P.; Yang, W.-Z.; Yuan, H. S.; Lim, C. Multi-Targeting of Functional Cysteines in Multiple Conserved SARS-CoV-2 Domains by Clinically Safe Zn-Ejectors. *Chem. Sci.* **2020**, *11*, 9904–9909.
- (129) Sies, H.; Parnham, M. J. Potential Therapeutic Use of Ebselen for COVID-19 and Other Respiratory Viral Infections. *Free Radical Biol. Med.* **2020**, *156*, 107–112.
- (130) Menéndez, C. A.; Byléhn, F.; Perez-Lemus, G. R.; Alvarado, W.; de Pablo, J. J. Molecular Characterization of Ebselen Binding Activity to SARS-CoV-2 Main Protease. *Sci. Adv.* **2020**, *6*, eabd3045.
- (131) Aebischer, D.; Greer, A. Extreme Sulfur Chemistry. *J. Sulfur Chem.* **2008**, *29*, 241–241.
- (132) Barton, P.; Hunter, C. A.; Potter, T. J.; Webb, S. J.; Williams, N. H. Transmembrane Signalling. *Angew. Chem., Int. Ed.* **2002**, *41*, 3878–3881.
- (133) Dado, G. P.; Gellman, S. H. Redox Control of Secondary Structure in a Designed Peptide. *J. Am. Chem. Soc.* **1993**, *115*, 12609–12610.
- (134) Míšek, J.; Vargas Jentsch, A.; Sakurai, S.; Emery, D.; Mareda, J.; Matile, S. A Chiral and Colorful Redox Switch: Enhanced  $\pi$  Acidity in Action. *Angew. Chem., Int. Ed.* **2010**, *49*, 7680–7683.
- (135) Strakova, K.; Assies, L.; Goujon, A.; Piazzolla, F.; Humeniuk, H. V.; Matile, S. Dithienothiophenes at Work: Access to Mechanosensitive Fluorescent Probes, Chalcogen-Bonding Catalysis, and Beyond. *Chem. Rev.* **2019**, *119*, 10977–11005.
- (136) Deming, T. J. Functional Modification of Thioether Groups in Peptides, Polypeptides, and Proteins. *Bioconjugate Chem.* **2017**, *28*, 691–700.
- (137) Donnelly, D. P.; Dowgiallo, M. G.; Salisbury, J. P.; Aluri, K. C.; Iyengar, S.; Chaudhari, M.; Mathew, M.; Miele, I.; Auclair, J. R.; Lopez, S. A.; Manetsch, R.; Agar, J. N. Cyclic Thiosulfonates and Cyclic Disulfides Selectively Cross-Link Thiols While Avoiding Modification of Lone Thiols. *J. Am. Chem. Soc.* **2018**, *140*, 7377–7380.
- (138) Donnelly, D. P.; Agar, J. N.; Lopez, S. A. Nucleophilic Substitution Reactions of Cyclic Thiosulfonates Are Accelerated by Hyperconjugative Interactions. *Chem. Sci.* **2019**, *10*, 5568–5575.
- (139) Ferreira, R. B.; Law, M. E.; Jahn, S. C.; Davis, B. J.; Heldermon, C. D.; Reinhard, M.; Castellano, R. K.; Law, B. K. Novel Agents That Downregulate EGFR, HER2, and HER3 in Parallel. *Oncotarget* **2015**, *6*, 10445–10459.

- (140) Qing, Y.; Ionescu, S. A.; Pulcu, G. S.; Bayley, H. Directional Control of a Processive Molecular Hopper. *Science* **2018**, *361*, 908–912.
- (141) Pulcu, G. S.; Mikhailova, E.; Choi, L.-S.; Bayley, H. Continuous Observation of the Stochastic Motion of an Individual Small-Molecule Walker. *Nat. Nanotechnol.* **2015**, *10*, 76–83.
- (142) Moaven, S.; Watson, B. T.; Thompson, S. B.; Lyons, V. J.; Unruh, D. K.; Casadonte, D. J.; Pappas, D.; Cozzolino, A. F. Self-Assembly of Reversed Bilayer Vesicles through Pnictogen Bonding: Water-Stable Supramolecular Nanocontainers for Organic Solvents. *Chem. Sci.* **2020**, *11*, 4374–4380.
- (143) Griffin, B. A.; Adams, S. R.; Tsien, R. Y. Specific Covalent Labeling of Recombinant Protein Molecules Inside Live Cells. *Science* **1998**, *281*, 269–272.
- (144) Walker, A. S.; Rablen, P. R.; Schepartz, A. Rotamer-Restricted Fluorogenicity of the Bis-Arsenical ReAsH. *J. Am. Chem. Soc.* **2016**, *138*, 7143–7150.
- (145) Gini, A.; Paraja, M.; Galmés, B.; Besnard, C.; Poblador-Bahamonde, A. I.; Sakai, N.; Frontera, A.; Matile, S. Pnictogen-Bonding Catalysis: Brevetoxin-Type Polyether Cyclizations. *Chem. Sci.* **2020**, *11*, 7086–7091.
- (146) Lloyd, N. C.; Morgan, H. W.; Nicholson, B. K.; Ronimus, R. S. The Composition of Ehrlich's Salvarsan: Resolution of a Century-Old Debate. *Angew. Chem., Int. Ed.* **2005**, *44*, 941–944.
- (147) Campaña, A. G.; Leigh, D. A.; Lewandowska, U. One-Dimensional Random Walk of a Synthetic Small Molecule toward a Thermodynamic Sink. *J. Am. Chem. Soc.* **2013**, *135*, 8639–8645.
- (148) Zhong, Y.; Xu, Y.; Anslyn, E. V. Studies of Reversible Conjugate Additions. *Eur. J. Org. Chem.* **2013**, *2013*, 5017–5021.
- (149) Bravin, C.; Hunter, C. A. Template Effects of Vesicles in Dynamic Covalent Chemistry. *Chem. Sci.* **2020**, *11*, 9122–9125.
- (150) Jiang, X.; Yu, Y.; Chen, J.; Zhao, M.; Chen, H.; Song, X.; Matzuk, A. J.; Carroll, S. L.; Tan, X.; Sizovs, A.; Cheng, N.; Wang, M. C.; Wang, J. Quantitative Imaging of Glutathione in Live Cells Using a Reversible Reaction-Based Ratiometric Fluorescent Probe. *ACS Chem. Biol.* **2015**, *10*, 864–874.
- (151) Hill, T.; Odell, L. R.; Edwards, J. K.; Graham, M. E.; McGeachie, A. B.; Rusak, J.; Quan, A.; Abagyan, R.; Scott, J. L.; Robinson, P. J.; McCluskey, A. Small Molecule Inhibitors of Dynamin I GTPase Activity: Development of Dimeric Tyrphostins. *J. Med. Chem.* **2005**, *48*, 7781–7788.
- (152) Macpherson, L. J.; Dubin, A. E.; Evans, M. J.; Marr, F.; Schultz, P. G.; Cravatt, B. F.; Patapoutian, A. Noxious Compounds Activate TRPA1 Ion Channels through Covalent Modification of Cysteines. *Nature* **2007**, *445*, 541–545.
- (153) Núñez-Villanueva, D.; Hunter, C. A. Replication of Sequence Information in Synthetic Oligomers. *Acc. Chem. Res.* **2021**, *54*, 1298–1306.
- (154) Sadownik, A.; Stefely, J.; Regen, S. L. Polymerized Liposomes Formed under Extremely Mild Conditions. *J. Am. Chem. Soc.* **1986**, *108*, 7789–7791.
- (155) Kisanuki, A.; Kimpara, Y.; Oikado, Y.; Kado, N.; Matsumoto, M.; Endo, K. Ring-Opening Polymerization of Lipoic Acid and Characterization of the Polymer. *J. Polym. Sci., Part A: Polym. Chem.* **2010**, *48*, 5247–5253.
- (156) Zhang, X.; Waymouth, R. M. 1,2-Dithiolane-Derived Dynamic, Covalent Materials: Cooperative Self-Assembly and Reversible Cross-Linking. *J. Am. Chem. Soc.* **2017**, *139*, 3822–3833.
- (157) Margulis, K.; Zhang, X.; Joubert, L.-M.; Bruening, K.; Tassone, C. J.; Zare, R. N.; Waymouth, R. M. Formation of Polymeric Nanocubes by Self-Assembly and Crystallization of Dithiolane-Containing Triblock Copolymers. *Angew. Chem., Int. Ed.* **2017**, *56*, 16357–16362.
- (158) Barcan, G. A.; Zhang, X.; Waymouth, R. M. Structurally Dynamic Hydrogels Derived from 1,2-Dithiolanes. *J. Am. Chem. Soc.* **2015**, *137*, 5650–5653.
- (159) Zhang, Q.; Deng, Y.-X.; Luo, H.-X.; Shi, C.-Y.; Geise, G. M.; Feringa, B. L.; Tian, H.; Qu, D.-H. Assembling a Natural Small Molecule into a Supramolecular Network with High Structural Order and Dynamic Functions. *J. Am. Chem. Soc.* **2019**, *141*, 12804–12814.
- (160) Zhang, Q.; Deng, Y.; Shi, C.-Y.; Feringa, B. L.; Tian, H.; Qu, D.-H. Dual Closed-Loop Chemical Recycling of Synthetic Polymers by Intrinsically Reconfigurable Poly(disulfides). *Matter* **2021**, *4*, 1352–1364.
- (161) Deng, Y.; Zhang, Q.; Feringa, B. L.; Tian, H.; Qu, D.-H. Toughening a Self-Healable Supramolecular Polymer by Ionic Cluster-Enhanced Iron-Carboxylate Complexes. *Angew. Chem., Int. Ed.* **2020**, *59*, 5278–5283.
- (162) Liu, F.; Wang, M.; Wang, Z.; Zhang, X. Polymerized Surface Micelles Formed under Mild Conditions. *Chem. Commun.* **2006**, *42*, 1610–1612.
- (163) Zhang, Z.; Liu, Q.; Sun, Z.; Phillips, B. K.; Wang, Z.; Al-Hashimi, M.; Fang, L.; Olson, M. A. Poly-Lipoic Ester-Based Coacervates for the Efficient Removal of Organic Pollutants from Water and Increased Point-of-Use Versatility. *Chem. Mater.* **2019**, *31*, 4405–4417.
- (164) Xu, H.; Cao, W.; Zhang, X. Selenium-Containing Polymers: Promising Biomaterials for Controlled Release and Enzyme Mimics. *Acc. Chem. Res.* **2013**, *46*, 1647–1658.
- (165) Chuard, N.; Fujisawa, K.; Morelli, P.; Saarbach, J.; Winsinger, N.; Metrangolo, P.; Resnati, G.; Sakai, N.; Matile, S. Activation of Cell-Penetrating Peptides with Ionpair- $\pi$  Interactions and Fluorophiles. *J. Am. Chem. Soc.* **2016**, *138*, 11264–11271.
- (166) Yafuso, M.; Kennedy, S. J.; Freeman, A. R. Spontaneous Conductance Changes, Multilevel Conductance States and Negative Differential Resistance in Oxidized Cholesterol Black Lipid Membranes. *J. Membr. Biol.* **1974**, *17*, 201–212.
- (167) Mosgaard, L. D.; Heimbürg, T. Lipid Ion Channels and the Role of Proteins. *Acc. Chem. Res.* **2013**, *46*, 2966–2976.
- (168) Colombini, M. Ceramide Channels. *Adv. Exp. Med. Biol.* **2019**, *1159*, 33–48.
- (169) Matsuzaki, K.; Murase, O.; Fujii, N.; Miyajima, K. An Antimicrobial Peptide, Magainin 2, Induced Rapid Flip-Flop of Phospholipids Coupled with Pore Formation and Peptide Translocation. *Biochemistry* **1996**, *35*, 11361–11368.
- (170) Göpflich, K.; Li, C.-Y.; Mames, I.; Bhamidimarri, S. P.; Ricci, M.; Yoo, J.; Mames, A.; Ohmann, A.; Winterhalter, M.; Stulz, E.; Aksimentiev, A.; Keyser, U. F. Ion Channels Made from a Single Membrane-Spanning DNA Duplex. *Nano Lett.* **2016**, *16*, 4665–4669.
- (171) Herce, H. D.; Garcia, A. E.; Litt, J.; Kane, R. S.; Martin, P.; Enrique, N.; Rebolledo, A.; Milesi, V. Arginine-Rich Peptides Destabilize the Plasma Membrane, Consistent with a Pore Formation Translocation Mechanism of Cell-Penetrating Peptides. *Biophys. J.* **2009**, *97*, 1917–1925.
- (172) Schmidt, D.; Jiang, Q.-X.; MacKinnon, R. Phospholipids and the Origin of Cationic Gating Charges in Voltage Sensors. *Nature* **2006**, *444*, 775–779.
- (173) Abegg, D.; Gasparini, G.; Hoch, D. G.; Shuster, A.; Bartolami, E.; Matile, S.; Adibekian, A. Strained Cyclic Disulfides Enable Cellular Uptake by Reacting with the Transferrin Receptor. *J. Am. Chem. Soc.* **2017**, *139*, 231–238.
- (174) Daniels, T. R.; Delgado, T.; Helguera, G.; Penichet, M. L. The Transferrin Receptor Part II: Targeted Delivery of Therapeutic Agents into Cancer Cells. *Clin. Immunol.* **2006**, *121*, 159–176.
- (175) Wessling-Resnick, M. Crossing the Iron Gate: Why and How Transferrin Receptors Mediate Viral Entry. *Annu. Rev. Nutr.* **2018**, *38*, 431–458.
- (176) Tang, X.; Yang, M.; Duan, Z.; Liao, Z.; Liu, L.; Cheng, R.; Fang, M.; Wang, G.; Liu, H.; Xu, J.; Kamau, P. M.; Zhang, Z.; Yang, L.; Zhao, X.; Peng, X.; Lai, R. Transferrin Receptor Is Another Receptor for SARS-CoV-2 Entry. *bioRxiv* **2020**, DOI: 10.1101/2020.10.23.350348.
- (177) Littler, D. R.; Harrop, S. J.; Goodchild, S. C.; Phang, J. M.; Mynott, A. V.; Jiang, L.; Valenzuela, S. M.; Mazzanti, M.; Brown, L. J.; Breit, S. N.; Curmi, P. M. G. The Enigma of the CLIC Proteins: Ion Channels, Redox Proteins, Enzymes, Scaffolding Proteins? *FEBS Lett.* **2010**, *584*, 2093–2101.

- (178) Singh, H. Two Decades with Dimorphic Chloride Intracellular Channels (CLICs). *FEBS Lett.* **2010**, *584*, 2112–2121.
- (179) Argenzio, E.; Moolenaar, W. H. Emerging Biological Roles of Cl<sup>-</sup> Intracellular Channel Proteins. *J. Cell Sci.* **2016**, *129*, 4165–4174.
- (180) Singh, H.; Ashley, R. H. Redox Regulation of CLIC1 by Cysteine Residues Associated with the Putative Channel Pore. *Biophys. J.* **2006**, *90*, 1628–1638.
- (181) Khamici, H. A.; Brown, L. J.; Hossain, K. R.; Hudson, A. L.; Sinclair-Burton, A. A.; Ng, J. P. M.; Daniel, E. L.; Hare, J. E.; Cornell, B. A.; Curmi, P. M. G.; Davey, M. W.; Valenzuela, S. M. Members of the Chloride Intracellular Ion Channel Protein Family Demonstrate Glutaredoxin-Like Enzymatic Activity. *PLoS One* **2015**, *10*, e115699.
- (182) Bethel, N. P.; Grabe, M. Atomistic Insight into Lipid Translocation by a TMEM16 Scramblase. *Proc. Natl. Acad. Sci. U. S. A.* **2016**, *113*, 14049–14054.
- (183) Alvardia, C.; Lim, N. K.; Clerico Mosina, V.; Oostergetel, G. T.; Dutzler, R.; Paulino, C. Cryo-EM Structures and Functional Characterization of the Murine Lipid Scramblase TMEM16F. *eLife* **2019**, *8*, e44365.
- (184) Feng, S.; Dang, S.; Han, T. W.; Ye, W.; Jin, P.; Cheng, T.; Li, J.; Jan, Y. N.; Jan, L. Y.; Cheng, Y. Cryo-EM Studies of TMEM16F Calcium-Activated Ion Channel Suggest Features Important for Lipid Scrambling. *Cell Rep.* **2019**, *28*, 567–579.
- (185) Han, T. W.; Ye, W.; Bethel, N. P.; Zubia, M.; Kim, A.; Li, K. H.; Burlingame, A. L.; Grabe, M.; Jan, Y. N.; Jan, L. Y. Chemically Induced Vesiculation as a Platform for Studying TMEM16F Activity. *Proc. Natl. Acad. Sci. U. S. A.* **2019**, *116*, 1309–1318.
- (186) Paulsen, C. E.; Armache, J.-P.; Gao, Y.; Cheng, Y.; Julius, D. Structure of the TRPA1 Ion Channel Suggests Regulatory Mechanisms. *Nature* **2015**, *520*, 511–517.
- (187) Muralidharan, P.; Cserne Szappanos, H.; Ingley, E.; Hool, L. Evidence for Redox Sensing by a Human Cardiac Calcium Channel. *Sci. Rep.* **2016**, *6*, 19067.
- (188) Jiménez-Vidal, M.; Gasol, E.; Zorzano, A.; Nunes, V.; Palacín, M.; Chillarón, J. Thiol Modification of Cysteine 327 in the Eighth Transmembrane Domain of the Light Subunit XCT of the Heteromeric Cystine/Glutamate Antiporter Suggests Close Proximity to the Substrate Binding Site/Permeation Pathway. *J. Biol. Chem.* **2004**, *279*, 11214–11221.
- (189) Tanaka, K.; Zhou, F.; Kuze, K.; You, G. Cysteine Residues in the Organic Anion Transporter MOAT1. *Biochem. J.* **2004**, *380*, 283–287.
- (190) Tomas, A.; Futter, C. E.; Eden, E. R. EGF Receptor Trafficking: Consequences for Signaling and Cancer. *Trends Cell Biol.* **2014**, *24*, 26–34.
- (191) Mansour, T. S.; Potluri, V.; Palapati, R. R.; Basetti, V.; Keesara, M.; Moghudula, A. G.; Maiti, P. Lead Generation of 1,2-Dithiolanes as Exon 19 and Exon 21 Mutant EGFR Tyrosine Kinase Inhibitors. *Bioorg. Med. Chem. Lett.* **2019**, *29*, 1435–1439.
- (192) Arosio, D.; Casagrande, C. Advancement in Integrin Facilitated Drug Delivery. *Adv. Drug Delivery Rev.* **2016**, *97*, 111–143.
- (193) Lechner, C.; Jelkmann, M.; Bernkop-Schnürch, A. Thiolated Polymers: Bioinspired Polymers Utilizing One of the Most Important Bridging Structures in Nature. *Adv. Drug Delivery Rev.* **2019**, *151–152*, 191–221.
- (194) Kapadia, S. B.; Barth, H.; Baumert, T.; McKeating, J. A.; Chisari, F. V. Initiation of Hepatitis C Virus Infection Is Dependent on Cholesterol and Cooperativity between CD81 and Scavenger Receptor B Type I. *J. Virol.* **2007**, *81*, 374–383.
- (195) Fraser, J.; Boo, I.; Pountourios, P.; Drummer, H. E. Hepatitis C Virus (HCV) Envelope Glycoproteins E1 and E2 Contain Reduced Cysteine Residues Essential for Virus Entry. *J. Biol. Chem.* **2011**, *286*, 31984–31992.
- (196) Turano, C.; Coppari, S.; Altieri, F.; Ferraro, A. Proteins of the PDI Family: Unpredicted Non-ER Locations and Functions. *J. Cell. Physiol.* **2002**, *193*, 154–163.
- (197) Soares Moretti, A. I.; Martins Laurindo, F. R. Protein Disulfide Isomerases: Redox Connections in and out of the Endoplasmic Reticulum. *Arch. Biochem. Biophys.* **2017**, *617*, 106–119.
- (198) Bi, S.; Hong, P. W.; Lee, B.; Baum, L. G. Galectin-9 Binding to Cell Surface Protein Disulfide Isomerase Regulates the Redox Environment to Enhance T-Cell Migration and HIV Entry. *Proc. Natl. Acad. Sci. U. S. A.* **2011**, *108*, 10650–10655.
- (199) Suhail, S.; Zajac, J.; Fossum, C.; Lowater, H.; McCracken, C.; Severson, N.; Laatsch, B.; Narkiewicz-Jodko, A.; Johnson, B.; Liebau, J.; Bhattacharyya, S.; Hati, S. Role of Oxidative Stress on SARS-CoV (SARS) and SARS-CoV-2 (COVID-19) Infection: A Review. *Protein J.* **2020**, *39*, 644–656.
- (200) Abell, B. A.; Brown, D. T. Sindbis Virus Membrane Fusion Is Mediated by Reduction of Glycoprotein Disulfide Bridges at the Cell Surface. *J. Virol.* **1993**, *67*, 5496–5501.
- (201) Glomb-Reinmund, S.; Kielian, M. The Role of Low pH and Disulfide Shuffling in the Entry and Fusion of Semliki Forest Virus and Sindbis Virus. *Virology* **1998**, *248*, 372–381.
- (202) Faaberg, K. S.; Even, C.; Palmer, G. A.; Plegemann, P. G. Disulfide Bonds between Two Envelope Proteins of Lactate Dehydrogenase-Elevating Virus Are Essential for Viral Infectivity. *J. Virol.* **1995**, *69*, 613–617.
- (203) Gallagher, T. M. Murine Coronavirus Membrane Fusion Is Blocked by Modification of Thiols Buried within the Spike Protein. *J. Virol.* **1996**, *70*, 4683–4690.
- (204) Lavillette, D.; Barbouche, R.; Yao, Y.; Boson, B.; Cosset, F.-L.; Jones, I. M.; Fenouillet, E. Significant Redox Insensitivity of the Functions of the SARS-CoV Spike Glycoprotein - Comparison with HIV Envelope. *J. Biol. Chem.* **2006**, *281*, 9200–9204.
- (205) Fenouillet, E.; Barbouche, R.; Jones, I. M. Cell Entry by Enveloped Viruses: Redox Considerations for HIV and SARS-Coronavirus. *Antioxid. Redox Signaling* **2007**, *9*, 1009–1034.
- (206) Pinter, A.; Kopelman, R.; Li, Z.; Kayman, S. C.; Sanders, D. A. Localization of the Labile Disulfide Bond between SU and TM of the Murine Leukemia Virus Envelope Protein Complex to a Highly Conserved CWLC Motif in SU That Resembles the Active-Site Sequence of Thiol-Disulfide Exchange Enzymes. *J. Virol.* **1997**, *71*, 8073–8077.
- (207) Wallin, M.; Löving, R.; Ekström, M.; Li, K.; Garoff, H. Kinetic Analyses of the Surface-Transmembrane Disulfide Bond Isomerization-Controlled Fusion Activation Pathway in Moloney Murine Leukemia Virus. *J. Virol.* **2005**, *79*, 13856–13864.
- (208) Markovic, I.; Pulyaeva, H.; Sokoloff, A.; Chernomordik, L. V. Membrane Fusion Mediated by Baculovirus Gp64 Involves Assembly of Stable Gp64 Trimers into Multiprotein Aggregates. *J. Cell Biol.* **1998**, *143*, 1155–1166.
- (209) Jain, S.; McGinnes, L. W.; Morrison, T. G. Thiol/Disulfide Exchange Is Required for Membrane Fusion Directed by the Newcastle Disease Virus Fusion Protein. *J. Virol.* **2007**, *81*, 2328–2339.
- (210) Abou-Jaoudé, G.; Sureau, C. Entry of Hepatitis Delta Virus Requires the Conserved Cysteine Residues of the Hepatitis B Virus Envelope Protein Antigenic Loop and Is Blocked by Inhibitors of Thiol-Disulfide Exchange. *J. Virol.* **2007**, *81*, 13057–13066.
- (211) Mandel, R.; Ryser, H. J.-P.; Ghani, F.; Wu, M.; Peak, D. Inhibition of a Reductive Function of the Plasma Membrane by Bacitracin and Antibodies against Protein Disulfide-Isomerase. *Proc. Natl. Acad. Sci. U. S. A.* **1993**, *90*, 4112–4116.
- (212) Falnes, P. Ø.; Olsnes, S. Cell-Mediated Reduction and Incomplete Membrane Translocation of Diphtheria Toxin Mutants with Internal Disulfides in the A Fragment. *J. Biol. Chem.* **1995**, *270*, 20787–20793.
- (213) Spooner, R. A.; Watson, P. D.; Marsden, C. J.; Smith, D. C.; Moore, K. A. H.; Cook, J. P.; Lord, J. M.; Roberts, L. M. Protein Disulfide-Isomerase Reduces Ricin to Its A and B Chains in the Endoplasmic Reticulum. *Biochem. J.* **2004**, *383*, 285–293.
- (214) Orlandi, P. A. Protein-Disulfide Isomerase-Mediated Reduction of the A Subunit of Cholera Toxin in a Human Intestinal Cell Line. *J. Biol. Chem.* **1997**, *272*, 4591–4599.
- (215) McKee, M. L.; FitzGerald, D. J. Reduction of Furin-Nicked Pseudomonas Exotoxin A: An Unfolding Story. *Biochemistry* **1999**, *38*, 16507–16513.

(216) Jacquez, P.; Avila, G.; Boone, K.; Altiyev, A.; Puschhof, J.; Sauter, R.; Arigi, E.; Ruiz, B.; Peng, X.; Almeida, I.; Sherman, M.; Xiao, C.; Sun, J. The Disulfide Bond Cys255-Cys279 in the Immunoglobulin-Like Domain of Anthrax Toxin Receptor 2 Is Required for Membrane Insertion of Anthrax Protective Antigen Pore. *PLoS One* **2015**, *10*, e0130832.

(217) Flores, B. M.; Batzer, M. A.; Stein, M. A.; Petersen, C.; Diedrich, D. L.; Torian, B. E. Structural Analysis and Demonstration of the 29 KDa Antigen of Pathogenic *Entamoeba histolytica* as the Major Accessible Free Thiol-Containing Surface Protein. *Mol. Microbiol.* **1993**, *7*, 755–763.

(218) Raulston, J. E.; Davis, C. H.; Paul, T. R.; Hobbs, J. D.; Wyrick, P. B. Surface Accessibility of the 70-Kilodalton *Chlamydia trachomatis* Heat Shock Protein Following Reduction of Outer Membrane Protein Disulfide Bonds. *Infect. Immun.* **2002**, *70*, 535–543.

(219) Davis, C. H.; Raulston, J. E.; Wyrick, P. B. Protein Disulfide Isomerase, a Component of the Estrogen Receptor Complex, Is Associated with *Chlamydia trachomatis* Serovar E Attached to Human Endometrial Epithelial Cells. *Infect. Immun.* **2002**, *70*, 3413–3418.

(220) Naguleswaran, A.; Alaeddine, F.; Guionaud, C.; Vonlaufen, N.; Sonda, S.; Jenoe, P.; Mevissen, M.; Hemphill, A. Neospora Caninum Protein Disulfide Isomerase Is Involved in Tachyzoite-Host Cell Interaction. *Int. J. Parasitol.* **2005**, *35*, 1459–1472.

(221) Conant, C. G.; Stephens, R. S. *Chlamydia* Attachment to Mammalian Cells Requires Protein Disulfide Isomerase. *Cell. Microbiol.* **2007**, *9*, 222–232.

(222) Pacello, F.; D'Orazio, M.; Battistoni, A. An ERp57-Mediated Disulfide Exchange Promotes the Interaction between *Burkholderia cenocepacia* and Epithelial Respiratory Cells. *Sci. Rep.* **2016**, *6*, 21140.

(223) Moncada, D.; Arenas, A.; Acosta, A.; Molina, D.; Hernández, A.; Cardona, N.; Gomez-Yepes, M.; Gomez-Marin, J. E. Role of the 52 KDa Thioredoxin Protein Disulfide Isomerase of *Toxoplasma gondii* during Infection to Human Cells. *Exp. Parasitol.* **2016**, *164*, 36–42.

(224) Shang, J.; Wan, Y.; Luo, C.; Ye, G.; Geng, Q.; Auerbach, A.; Li, F. Cell Entry Mechanisms of SARS-CoV-2. *Proc. Natl. Acad. Sci. U. S. A.* **2020**, *117*, 11727–11734.

(225) Hoffmann, M.; Kleine-Weber, H.; Schroeder, S.; Krüger, N.; Herrler, T.; Erichsen, S.; Schiergens, T. S.; Herrler, G.; Wu, N.-H.; Nitsche, A.; Müller, M. A.; Drosten, C.; Pöhlmann, S. SARS-CoV-2 Cell Entry Depends on ACE2 and TMPRSS2 and Is Blocked by a Clinically Proven Protease Inhibitor. *Cell* **2020**, *181*, 271–280.

(226) Cantuti-Castelvetri, L.; Ojha, R.; Pedro, L. D.; Djannatian, M.; Franz, J.; Kuivanen, S.; Meer, F.; Kallio, K.; Kaya, T.; Anastasina, M.; Smura, T.; Levanov, L.; Szirovicza, L.; Tobi, A.; Kallio-Kokko, H.; Österlund, P.; Joensuu, M.; Meunier, F. A.; Butcher, S. J.; Winkler, M. S.; Mollenhauer, B.; Helenius, A.; Gokce, O.; Teesalu, T.; Hepojoki, J.; Vapalahti, O.; Stadelmann, C.; Balistreri, G.; Simons, M. Neuropilin-1 Facilitates SARS-CoV-2 Cell Entry and Infectivity. *Science* **2020**, *370*, 856–860.

(227) Rice, W. G.; Supko, J. G.; Malspeis, L.; Buckheit, R. W.; Clanton, D.; Bu, M.; Graham, L.; Schaeffer, C. A.; Turpin, J. A.; Domagala, J.; Gogliotti, R.; Bader, J. P.; Halliday, S. M.; Coren, L.; Sowder, R. C.; Arthur, L. O.; Henderson, L. E. Inhibitors of HIV Nucleocapsid Protein Zinc Fingers as Candidates for the Treatment of AIDS. *Science* **1995**, *270*, 1194–1197.